Supplement of Biogeosciences, 21, 4413–4437, 2024
https://doi.org/10.5194/bg-21-4413-2024-supplement

Supplement of

Palaeoecology of ungulates in northern Iberia during the Late Pleistocene through isotopic analysis of teeth

Mónica Fernández-García et al.

Correspondence to: Mónica Fernández-García (monica.fegar@gmail.com) and Ana B. Marín-Arroyo (anabelen.marin@unican.es)

Section S1. Sites description

S1.1. Vasco-Cantabrian sites

Axlor (Dima, Vizcaya, País Vasco)

Axlor is a rock-shelter located in Dima (43.2706; -1.8905), with a continuous Middle Paleolithic sequence from the MIS5 to the MIS3 (DeMuro et al., 2023; Pederzani et al., 2023; Marín-Arroyo et al., 2018). It is placed on the southwestern slope of the Dima Valley, with an elevation of approximately 320 m above sea level (a.s.l.), at 33 km straight from the present-day coastline, next to one of the lowest mountain passes linking the Cantabrian basins and the Alavese Plateau. The site was discovered in 1932 and initial excavations were performed by Barandiarán (1967-1974). J. M. Barandiarán undertook the excavations between 1967 and 1974, identifying eight Mousterian levels (I-VIII) (Barandiarán, 1980).

From 2000 to 2008, new excavations by González-Urquijo, Ibáñez-Estévez and Rios-Garaizar were achieved and, since 2019, these are ongoing by González-Urquijo and Lazuén. Due to the lack of chronology during Barandiarán excavations, among other aspects, work was focused on obtaining a detailed stratigraphy on the new excavation areas to correlate it with Barandiarán's levels (González-Urquijo & Ibáñez-Estévez, 2021; González Urquijo et al., 2005). The new stratigraphic sequence is roughly equivalent to the previous one, but with additional levels not previously identified or excavated by Barandiarán. Some of these levels were deposited before Level VIII (Gómez-Olivencia et al., 2018; 2020). The Middle Paleolithic sequence extends from layers VIII to III (or from N to B-C). Levallois production is predominant in the lower levels (VI to VIII), while Quina Mousterian technocomplex does in the upper ones (from III to V) (Rios-Garaizar, 2012, 2017). Recent chronological data by radiocarbon (Pederzani et al., 2023; Marín-Arroyo et al., 2018) and OSL (Demuro et al., 2023) methods confirm that a sequence Axlor levels VI, VIII, and VIII probably accumulated during MIS5d–a (109–82 ka), while levels D to B probably were formed during the period encompassing the start of MIS 4 (71–57 ka) through to the beginning or middle of MIS 3 (57–29 ka) and upper Level III to 46,200 ±3,000 BP, which calibrates between 45,350 cal BP and beyond the calibration curve at > 55,000 cal BP.

The archaeozoological study indicates an anthropic origin of the faunal assemblage with scarce carnivore activity documented (Altuna, 1989; Castaños, 2005; Gómez-Olivencia et al., 2018). In lower layers, the most abundant taxa are *Cervus elaphus* (VIII) and *Capra pyrenaica* (VII), while in upper layers III-V, C*ervus elaphus* is substituted by *Bos primigenious/Bison priscus* and *Equus sp*. The material included in this work comes from the faunal collection of the Barandiarán excavation currently curated at the Bizkaia Museum of Archaeology (Bilbao), where teeth were sampled, and the stable isotope analyses on enamel phosphate were included in Pederzani et al. (2023).

El Castillo (Puente Viesgo, Cantabria)

El Castillo cave is located in Puente Viesgo (43.2924; -3.9656), with an elevation of approximately 195m a.s.l., at 17 km straight from the present-day coastline. The cave belongs to the karstic system that was formed in the Monte Castillo, which dominates the Pas Valley. The site was discovered in 1903 by H. Alcalde del Río. H. Obermaier carried out the first excavation seasons between 1910 and 1914 when many of the archaeological remains were recovered, mainly from the cave hall. These interventions were done under the supervision of the "Institut de Paléontologie Humaine" (IPH) and Prince Albert I of Monaco. From 1980 to 2011, V. Cabrera and F. Bernaldo de Quirós underwent new excavations focusing on the cave entrance, on the Middle to Upper Paleolithic transitional levels, mainly 16, 18 and 20 (Cabrera-Valdes, 1984). The site has yielded an important stratigraphic sequence, composed by 26 sedimentological units (1-26) related to different anthropic occupational units, often separated by archaeologically sterile units: Eneolithic (2), Azilian (4), Magdalenian (6 and 8), Solutrean (10), Aurignacian (12, 14, 16 and 18), Mousterian (20, 21 and 22) and Acheulean (24) (Cabrera-Valdés, 1984).

Unit 21 is mostly sterile (Cabrera Valdés, 1984; Martín-Perea et al., 2023), and ESR dated it, yielding a mean date of 69,000 ± 9,200 years BP (Rink et al., 1997). However, Martín-Perea et al. (2023) suggested some dating uncertainty from interpreting the initial stratigraphic nomenclature. They suggest that the ESR dates provided for level 21 by Rink et al. (1997) were erroneously attributed to this unit and it might correspond to 20E, indicating that below that subunit, the chronology is older than 70,000 years BP (Martín-Perea et al., 2023). The Mousterian Unit 20 cave is divided into several subunits (Martín-Perea et al., 2023). In Unit 20, a cave roof collapse took place, transforming the cave system into an open rock shelter. This unit contains abundant archaeological and paleontological remains. Lithic industry consists of sidescrapers, denticulates, notches and cleavers, the majority on quartzite and presents both unifacial, bifacial discoid debitage and Levallois debitage. Unit 20E was attributed to Quina Mousterian by Sánchez-Fernández and Bernaldo De Quiros (2009) and contains a Neanderthal tooth (Garralda, 2005). Considering the geochronological uncertainties for dates on 20E related to Rink et al. (1997), we have decided to rely solely on ESR date of 47,000 ± 9400 BP provided by Liberda et al. (2010) for this level. Unit 20C presents clear evidence of the Mousterian lithic industry and radiocarbon dates of 48,700±3,400 uncal BP (OxA-22204) and 49,400±3,700 uncal BP (OxA-22205) (Wood et al., 2018) and mean ESR date of 42,700 ±9900 BP (Liberda et al., 2010). Level 19 is archaeologically sterile and separates Unit 20 from Unit 18 (Wood et al., 2018).

Unit 18 is divided into 18A (archaeologically sterile), 18B, and 18C. Levels 18B and 18C were classified as Transitional Aurignacian, representing a gradual transformation from the Mousterian to the Aurignacian, which is unique to El Castillo cave (Cabrera et al., 2001; Maíllo and Bernaldo de Quirós, 2010; Wood et al., 2018). These levels' dates and cultural attribution have been the subject of much debate (e.g. Zilhao and D'Errico, 2003; Wood et al., 2018). According to Wood et al. (2018), the last dates of these levels range between 42,000±1,500 uncal BP (OxA-22203) and 46,000±2,400 uncal BP (OxA-21973), which is much earlier than the start of the Aurignacian period in the Cantabrian region (Marín-Arroyo et al., 2018; Vidal-Cordasco et al., 2022). The lithic assemblage of Unit 18 appears to be dominated by Discoid/Levallois technology (Bernaldo de Quirós and Maíllo-Fernández, 2009) but with a high percentage of "Upper Paleolithic" pieces. Additionally, punctual bone industry and pieces with incisions and engravings were discovered in Unit 18 (Cabrera-Valdés et al., 2001). Three deciduous tooth crowns attributed to Neanderthals were found in Unit 18B (Garralda et al., 2022). Above, Unit 17 is sterile but contains scarce lithic and faunal materials, while Level 16 was attributed to the Proto-Aurignacian, with dates of 38,600±1,000 uncal BP (OxA-22200) (Wood et al., 2018).

According to Luret et al. (2020), there was a shift in hunting practices between the Late Mousterian (unit 20) and the Transitional Aurignacian (unit 18). During the Late Mousterian, hunting strategies were less specialized, and the species hunted included red deer, horses, and bovines. However, in Unit 18, a specialization in red deer hunting is observed. However, the explanation of this shift has been proposed as a response to a cultural choice or induced by climatic changes. However, recent taphonomic studies by Sanz-Royo et al. (2023) on the old collections of Aurignacian Delta level reveal a more significant role of carnivores than shown by Luret et al. (2020). The material included in this work comes from the faunal collection recovered during the Cabrera-Valdés and Bernaldo de Quirós excavations curated at Museo de Prehistoria y Arqueología de Cantabria (MUPAC, Santander).

Labeko Koba (Arrastre, Guipúzcoa, País Vasco)

Labeko Koba is a cave in the Kurtzetxiki Hill (43.0619; -2.4833), at 246 m a.s.l. and 29 km straight from the present-day Atlantic coast. In 1987 and 1988, the site was discovered due to the construction of the Arrasate ring road, and a savage excavation was carried out (Arrizabalaga, 2000a). Unfortunately, the site was destroyed after that. The stratigraphic sequence identified nine different levels. The lower Level IX was attributed to the Châtelperronian, based on the presence of three Châtelperron points. Although there is a lack of human remains in few Cantabrian Châtelperronian sites, recent research has suggested that this techno-complex was produced by Neanderthals (Maroto et al., 2012; Rios-Garaizar et al., 2022). Level VII marks the beginning of the Aurignacian sequence, likely Proto-Aurignacian, with a lithic assemblage dominated by Dufour bladelets (Arrizabalaga, 2000a). Levels VI, V, and IV contain lithic assemblages that suggested an Early Aurignacian attribution (Arrizabalaga, 2000b; Arrizabalaga et al., 2009). This site is significant because it is one of the few sites with Châtelperronian assemblages and with both Proto-Aurignacian and Early Aurignacian separated (Arrizabalaga et al., 2009).

Initial radiocarbon dates were inconsistent with the stratigraphy of the site and much more recent than expected for the Early Upper Paleolithic (Arrizabalaga, 2000a). This incoherence was determined to be affected by taphonomic alterations (Wood et al., 2014). Later radiocarbon dates undertaken with an ultrafiltration pre-treatment provided a new regional framework for the regional Early Upper Paleolithic (Wood et al., 2014). The Châtelperronian layer IX inf is dated to 38,100±900 uncal BP (OxA-22562) and 37,400±800 uncal BP (OxA-22560). The Proto-Aurignacian levels cover a period from 36,850±800 uncal BP (OxA-21766) to 35,250±650 uncal BP (OxA-21793). The three Early Aurignacian levels are dated to 35,100±600 uncal BP (OxA-21778) for level VI, ~ 34,000 uncal BP (OxA-21767 and OxA-21779) for level V, and ~ 33,000 BP (OxA-21768 and OxA-21780) for level IV (Arrizabalaga et al., 2009).

Taphonomic studies indicate an alternation in the use of the cave between carnivores and humans, the latter during short occupation periods (Villaluenda et al., 2012; Ríos-Garaizar et al., 2012; Arrizabalaga et al., 2010). Labeko Koba is considered to have functioned as a natural trap where carnivores, mainly hyenas, access animal carcasses. At least in the base of Labeko Koba IX, carnivore activity was higher, and they would have consumed the same prey as humans (Villaluenga et al., 2012). The presence of humans is linked to strategic use as a campsite associated with a small assemblage of lithic artifacts. The most consumed species by Châtelperronian groups were red deer, followed by the consumption of large bovids, equids, and woolly rhinoceros. During the Aurignacian period, there was some stability in human occupations, although they still alternated with carnivore occupations (Arrizabalaga et al., 2010). Cold-adapted fauna such as reindeer and woolly rhinoceros were identified in association with the Châtelperronian. Reindeer and the woolly mammoth and arctic fox were still present during the Aurignacian levels. The original sampling of the teeth studied by this work was performed in the San Sebastian Heritage Collection headquarters, where the Guipuzcoa archaeological materials were deposited at that time.

Aitzbitarte III interior (Rentería, Guipúzcoa, País Vasco)

Aitzbitarte III is an archaeological site located within the Landarbaso karstic system comprising nine caves (43.270; -1.8905). The cave is situated 220 m.a.s.l. and is 10 km away from the present-day coastline. Initial archaeological interventions were carried out at the end of the 19th century by P.M. de Soraluce (Altuna, 2011). Recent excavations were initially conducted in the deep zone inside the cave between 1986 and 1993, where the studied tooth was recovered, and later focused on the cave entrance between 1994 and 2002, by J. Altuna, K. Mariezkurrena, and J. Ríos-Garaizar (Altuna et al., 2011; 2017).

While the cave's entrance area contains a sequence comprising possible Mousterian and Evolved Aurignacian and Gravettian levels (Altuna et al., 2011; 2013), the stratigraphy in the inner cave presents eight levels: level VIII (some tools with Mousterian features), VII (sterile), VIb, VIa and V (Middle Gravettian technocomplex with abundance of Noailles burins), IV-II (disturbed archaeological levels) and I (surface) (Altuna et al., 2017). Levels V have dates of 24,910 uncal BP (I-15208) and 23,230 uncal BP (Ua-2243); whereas level VI extends from 23,830 ± 345 uncal BP (Ua-2628) and 25,380± 430 uncal BP (Ua-2244) (Altuna, 1992; Altuna et al., 2017), with a possible outlier dated at 21,130 uncal BP (Ua-1917).

The Gravettian occupation in the inner part of the cave was initially thought to be more recent than the one in the cave entrance. However, it was not easy to correlate the two excavation areas due to different sedimentation rates. The abundant human occupations took place during a singular cold phase in the Middle Gravettian with a specialized paleoeconomy focused on the hunting of *Bos primigenius* and *Bison priscus* (85% in level VI and 68% in level V), which is unusual in the Cantabrian region mostly focused on red deer and ibex. Other ungulates present are *Cervus elaphus* and *Rupicapra rupicapra*, and to a lesser extent *Capra pyrenaica, Capreolus capreolus, Rangifer tarandus*, and *Equus ferus* (Altuna et al., 2017; Altuna &

Mariezkurrena, 2020). There is a scarce representation of carnivores. The tooth studied was sampled at the Gordailua Center for Heritage Collections of the Provincial Council of Gipuzkoa.

El Otero (Secadura, Voto, Cantabria)

El Otero cave is located in Secadura (Voto) (43.3565; -3.5360), at 129 m.s.a.l and 12 km from the present-day coastline, near the Matienzo valley in a coastal plain environment covered by meadows and gentle hills. The discovery was made in 1908 by Lorenzo Sierra. The site was excavated in 1963 by J. Gonzalez Echegaray and M.A. García Guinea, in two different sectors (Sala I and Sala II) with an equivalent stratigraphic sequence (González Echegaray, 1966). Nine levels were identified in Sala I, from level IX to level I. Levels IX and VIII were initially related to the "Aurignacian-Mousterian, based on lithics assemblages with a combination of both technocomplex features. The overlying levels VI-IV were separated by a speleothem crust (level VII) and were initially related to Aurignacian, due to the presence of end-scrappers, bone points, blades, or burins on truncation (Freeman, 1964; Rios-Garaizar, 2013). Also, perforated deer, ibex, and fox teeth were found in levels V and IV. This site lacked chronological dating methods, until a selection of material from levels VI, V and IV revealed a difference in chrono-cultural attribution (Marín-Arroyo et al., 2018). Radiocarbon results yielded younger dates for such a cultural attribution and showed significant stratigraphic inconsistency. Level VI gave a result of 12,415±55 uncal BP (OxA-32585), two dates in Level V are 12,340±55 (OxA-32509) and 10,585±50 uncal BP (OxA-32510), and a date in Level IV is 15,990±80 uncal BP (OxA-32508). All these results fall into the range of the Late Upper Paleolithic (Magdalenian-Azilian initially identified in levels III-I), eliminating attribution of these levels to the Aurignacian despite the presence of apparently characteristic artefacts. Further assessments of archaeological materials will be needed.

Red deer dominate the assemblage, except for level IV where horses are more abundant. Wild boar, roe deer, and ibex are also present, but large bovids are relatively rare (González Echegaray, 1966). Level IV is the richest and most anthropogenic level, with evidence of butchering in red deer (captured in winter and early summer) and chamois (in autumn). The formation of this level involved humans and carnivores, and although certain data may suggest an anthropogenic predominance, the limited sample analyzed taphonomically and the pre-selection of preserved pieces do not allow for a definitive conclusion (Yravedra & Gómez-Castanedo, 2010). The material included in this work is curated at the Museo de Prehistoria y Arqueología de Cantabria (MUPAC, Santander).

S1.2. Northeastern Iberia sites

Terrasses de la Riera dels Canyars (Gavà, Barcelona, Cataluña)

Terrasses de la Riera dels Canyars (henceforth, Canyars) is an open-air site located near Gavà (Barcelona) (41.2961;1.9797), at 28 m.s.a.l and 3 km straight from the present-day coastline. The site lies on a fluvial terrace at the confluence of Riera dels Canyars, a torrential stream between Garraf Massif, Llobregat delta and Riera de Can Llong (Daura et al., 2013). Archaeo-paleontological remains were discovered during quarries activities in 2005 and was complete excavated on 2007 by the *Grup de Recerca del Quaternari* (Daura and Sanz, 2006; Daura et al., 2013). This intervention determined nine lithological units. The paleontological and archaeological remains come exclusively from one unit, the middle luthitic unit (MLU), and specifically from layer I. The MLU is composed of coarse sandy clays and gravels, filling a paleochannel network named lower detrital unit (LDU) (Daura et al., 2013). Five radiocarbon dates were obtained on charcoals from layer I, which yield statistically consistent ages from 33,800 ±350 uncal BP to 34,900 ±340 uncal BP, which results in mean age of 39,710 cal BP (from 40,890 to 38,530 cal BP) (Daura et al., 2013; this work).

The layer I of the site has yielded a rich faunal assemblage, consisting of over 5,000 remains. Among the herbivores, the most common species found are *Equus ferus*, *Bos primigenius, Equus hydruntinus*, and *Cervus elaphus* (Daura et al., 2013; Sanz-Royo et al., 2020). *Capra* sp. and *Sus scrofa are* also present, although in lower frequencies. The carnivores found at the site are also noteworthy, with *Crocuta crocuta* and *Lynx pardinus* being the most frequent. Presence of cold-adapted fauna associated to stepped environments is recorded, such as cf. *Mammuthus* sp., *Coelodonta antiquitatis*, and *Equus hydruntinus*. Small mammal analysis, pollen, and use-wear analysis have provided further evidence that a steppe-dominated landscape surrounded the Canyars site, supporting a correlation with the Heinrich Stadial 4, in coherence with the chronology obtained for the layer (López-García et al. 2013; 2023; Rivals et al., 2017). However, the presence of woodland is also attested by forest taxa within charcoal and pollen assemblages (Daura et al., 2013).

Taphonomic study is ongoing. But several evidences point that hyenas have played an important role in the accumulation of the faunal assemblage (Daura et al., 2013; Jimenez et al. 2019). However, sporadic human presence is documented by few human modifications found in faunal remains (cutmarks and fire alterations). Although the paucity of the lithic assemblage in the site, it shows a clear attribution to Upper Palaeolithic technocomplex, most likely the Early Aurignacian (Daura et al., 2013). Recently, it was documented a perforated bone fragment, which has been identified as a perforated board for leather production (Doyon et al., 2023). All teeth included in this work were sampled in *Laboratori de la Guixera* (Ajuntament de Casteldefels) where the material is stored.

References Section S1

Altuna, J. and Mariezkurrena, K.: Estrategias de caza en el Paleolítico superior de la Región Cantábrica., Sagvntvm, Extra 21, 219–225, 2020.

Altuna, J., Mariezkurrena, K., de la Peña, P., and Rios-Garaizar, J.: Ocupaciones Humanas En La Cueva de Aitzbitarte III (Renteria, País Vasco) Sector Entrada: 33.000-18.000 BP, Serv. Cent. Publicaciones del Gob. Vasco; EKOB, 11–21, 2011.

Altuna, J., Mariezkurrena, K., de la Peña, P., and Rios-Garaizar, J.: Los niveles gravetienses de la cueva de Aitzbitarte III (Gipuzkoa). Industrias y faunas asociada, in: Pensando El Gravetiense: Nuevos Datos Para La Región Cantábrica En Su Contexto Peninsular Y Pirenaico. Monografías Del Museo Nacional Y Centro de Investigación de Altamira, 23, 184–204, 2013.

Altuna, J., Mariezkurrena, K., Rios-Garaizar, J., and San Emeterio, A.: Ocupaciones Humanas en Aitzbitarte III (País Vasco) 26.000 - 13.000 BP (zona profunda de la cueva), Servicio Central de Publicaciones del Gobierno Vasco, 348 pp., 2017.

Arrizabalaga, A.: Los tecnocomplejos líticos del yacimiento arqueológico de Labeko Koba (Arrasate, País Vasco), in: Labeko Koba (País Vasco). Hienas y Humanos en los Albores del Paleolítico Superior, Munibe (Antropologia-Arkeologia) 52, edited by: Arrizabalaga, A. and Altuna, J., Sociedad de Ciencias Aranzadi, San Sebastián-Donostia, 193–343, 2000a.

Arrizabalaga, Á.: El yacimiento arqueológico de Labeko Koba (Arrasate, País Vasco). Entorno. Crónica de las investigaciones. Estratigrafía y estructuras. Cronología absoluta., in: Labeko Koba (País Vasco). Hienas y Humanos en los Albores del Paleolítico Superior, Munibe (Antropologia-Arkeologia) 52, edited by: Arrizabalaga, A. and Altuna, J., Sociedad de Ciencias Aranzadi, San Sebastián-Donostia, 15–72, 2000b.

Arrizabalaga, Á. and Rios-Garaizar, J.: The Early Aurignacian in the Basque Country, Quat. Int., 207, 25–36, 2009.

Arrizabalaga, Á., Iriarte-Chiapusso, M. J., and Villaluenga, A.: Labeko Koba y Lezetxiki (País Vasco). Dos yacimientos, una problemática común, Zo. Arqueol., 13, 322–334, 2010.

Barandiarán, J. M.: Excavaciones en Axlor. 1967- 1974, in: Obras Completas. Tomo XVII, edited by: Barandiarán, J. M., 341–359, 1980.

Bernaldo de Quirós, F. and Maillo-Fernández, J. M.: Middle to Upper Palaeolithic at Cantabrian Spain, in: A sourcebook of Palaeolithic transitions: methods, theories and interpretations, edited by: Camps, M. and Chauhan, P. R., Springer, New York, 341–359, 2009.

Cabrera, V., Maillo, J. M., Lloret, M., and Bernaldo de Quiros, F.: La transition vers le Paléolithique supérieur dans la grotte du Castillo (Cantabrie, Espagne) : la couche 18, Anthropologie., 105, 505–532, https://doi.org/10.1016/S0003-5521(01)80050-9, 2001.

Cabrera Valdés, V.: El Yacimiento de la cueva de «El Castillo» (Puente Viesgo, Santander), Bibliothec., CSIC, 485 pp., 1984.

Daura, J. and Sanz, M.: Informe de la troballa del jaciment arqueològic “Terrasses dels Canyars” (Castelldefels-Gavà). Notificació de la descoberta i propostes d’actuació. Grup de Recerca del Quaternari, SERP, UB, 2006.

Daura, J., Sanz, M., García, N., Allué, E., Vaquero, M., Fierro, E., Carrión, J. S., López-García, J. M., Blain, H. a., Sánchez-Marco, a., Valls, C., Albert, R. M., Fornós, J. J., Julià, R., Fullola, J. M., and Zilhão, J.: Terrasses de la Riera dels Canyars (Gavà, Barcelona): The landscape of Heinrich Stadial 4 north of the “ Ebro frontier” and implications for modern human dispersal into Iberia, Quat. Sci. Rev., 60, 26–48, https://doi.org/10.1016/j.quascirev.2012.10.042, 2013.

Demuro, M., Arnold, L. J., González-Urquijo, J., Lazuen, T., and Frochoso, M.: Chronological constraint of Neanderthal cultural and environmental changes in southwestern Europe: MIS 5–MIS 3 dating of the Axlor site (Biscay, Spain), J. Quat. Sci., 38, 891–920, https://doi.org/10.1002/jqs.3527, 2023.

Doyon, L., Faure, T., Sanz, M., Daura, J., Cassard, L., and D’Errico, F.: A 39,600-year-old leather punch board from Canyars, Gavà, Spain, Sci. Adv., 9, https://doi.org/10.1126/sciadv.adg0834, 2023.

Freeman, L. G.: Mousterian Developments in Cantabrian Spain, University of Chicago, 1964.

Garralda, M.-D.: Los Neandertales en la Península Ibérica:The Neandertals from the Iberian Peninsula, Munibe 57, 289–314, 2005.

Garralda, M.-D., Maíllo-Fernández, J.-M., Maureille, B., Neira, A., and de Quirós, F. B.: > 42 ka human teeth from El Castillo Cave (Cantabria, Spain) Mid-Upper Paleolithic transition, Archaeol. Anthropol. Sci., 14, 126, https://doi.org/10.1007/s12520-022-01587-2, 2022.

Gómez-Olivencia, A., Arceredillo, D., Álvarez-Lao, D. J., Garate, D., San Pedro, Z., Castaños, P., and Rios-Garaizar, J.: New evidence for the presence of reindeer (Rangifer tarandus) on the Iberian Peninsula in the Pleistocene: an archaeopalaeontological and chronological reassessment, Boreas, 43, 286–308, https://doi.org/10.1111/bor.12037, 2014.

Gómez-Olivencia, A., Sala, N., Núñez-Lahuerta, C., Sanchis, A., Arlegi, M., and Rios-Garaizar, J.: First data of Neandertal bird and carnivore exploitation in the Cantabrian Region (Axlor; Barandiaran excavations; Dima, Biscay, Northern Iberian Peninsula), Sci. Rep., 8, 10551, https://doi.org/10.1038/s41598-018-28377-y, 2018.

González-Urquijo, J.: Abrigo de Axlor (Dima)., Arkeoikuska, Investigac, 90–93, 2001.

González-Urquijo, J., Ibánez Estévez, J. J., Rios-Garaizar, J., Bourguignon, L., Castaños, P., and Tarriño Vinagre, A.: Excavaciones recientes en Axlor. Movilidad y planificación de actividades en grupos de neandertales, in: Actas de La Reunión Científica: Neandertales Cantábricos. Estado de La Cuestión. Monografías Del Museo Nacional Y Centro de Investigación de Altamira, 20, edited by: Montes Barquín, R. and Lasheras, J. A., Ministerio de Cultura, 527–539, 2005.

González Echegaray, J. G.: Cueva del Otero, Excavaciones Arqueol. en España, 53, 1966.

Jimenez, I. J., Sanz, M., Daura, J., De Gaspar, I., and García, N.: Ontogenetic dental patterns in Pleistocene hyenas (Crocuta crocuta Erxleben, 1777) and their palaeobiological implications, Int. J. Osteoarchaeol., 29, 808–821, https://doi.org/10.1002/oa.2796, 2019.

Liberda, J. J., Thompson, J. W., Rink, W. J., Bernaldo de Quirós, F., Jayaraman, R., Selvaretinam, K., Chancellor-Maddison, K., and Volterra, V.: ESR dating of tooth enamel in Mousterian layer 20, El Castillo, Spain, Geoarchaeology, n/a-n/a, https://doi.org/10.1002/gea.20320, 2010.

López-García, J. M., Blain, H.-A., Bennàsar, M., Sanz, M., and Daura, J.: Heinrich event 4 characterized by terrestrial proxies in southwestern Europe, Clim. Past, 9, 1053–1064, https://doi.org/10.5194/cp-9-1053-2013, 2013.

López-García, J. M., Blain, H. A., Fagoaga, A., Bandera, C. S., Sanz, M., and Daura, J.: Environment and climate during the Neanderthal-AMH presence in the Garraf Massif mountain range (northeastern Iberia) from the late Middle Pleistocene to Late Pleistocene inferred from small-vertebrate assemblages, Quat. Sci. Rev., 288, https://doi.org/10.1016/j.quascirev.2022.107595, 2022.

Luret, M., Burke, A., Bernaldo de Quiros, F., and Besse, M.: El Castillo cave (Cantabria, Spain): Archeozoological comparison between the Mousterian occupation level (unit 20) and the

"Aurignacien de transition de type El Castillo" (unit 18), J. Archaeol. Sci. Reports, 31, 102339, https://doi.org/10.1016/j.jasrep.2020.102339, 2020.

Marín-Arroyo, A. B., Rios-Garaizar, J., Straus, L. G., Jones, J. R., de la Rasilla, M., González Morales, M. R., Richards, M., Altuna, J., Mariezkurrena, K., and Ocio, D.: Chronological reassessment of the Middle to Upper Paleolithic transition and Early Upper Paleolithic cultures in Cantabrian Spain, PLoS One, 13, 1–20, https://doi.org/10.1371/journal.pone.0194708, 2018.

Maroto, J., Vaquero, M., Arrizabalaga, Á., Baena, J., Baquedano, E., Jordá, J., Julià, R., Montes, R., Van Der Plicht, J., Rasines, P., and Wood, R.: Current issues in late Middle Palaeolithic chronology: New assessments from Northern Iberia, Quat. Int., 247, 15–25, https://doi.org/10.1016/j.quaint.2011.07.007, 2012.

Martín-Perea, D. M., Maíllo-Fernández, J., Marín, J., Arroyo, X., and Asiaín, R.: A step back to move forward: a geological re-evaluation of the El Castillo Cave Middle Palaeolithic lithostratigraphic units (Cantabria, northern Iberia), J. Quat. Sci., 38, 221–234, https://doi.org/10.1002/jqs.3473, 2023.

Pederzani, S., Britton, K., Jones, J. R., Agudo Pérez, L., Geiling, J. M., and Marín-Arroyo, A. B.: Late Pleistocene Neanderthal exploitation of stable and mosaic ecosystems in northern Iberia shown by multi-isotope evidence, Quat. Res., 1–25, https://doi.org/10.1017/qua.2023.32, 2023.

Rink, W. J., Schwarcz, H. P., Lee, H. K., Cabrera Valdés, V., Bernaldo de Quirós, F., and Hoyos, M.: ESR dating of Mousterian levels at El Castillo Cave, Cantabria, Spain, J. Archaeol. Sci., 24, 593–600, https://doi.org/10.1006/jasc.1996.0143, 1997.

Rios-Garaizar, J.: Industria lítica y sociedad en la Transición del Paleolítico Medio al Superior en torno al Golfo de Bizkaia, PUbliCan - Ediciones de la Universidad de Cantabria, 432 pp., 2012.

Rios-Garaizar, J.: A new chronological and technological synthesis for Late Middle Paleolithic of the Eastern Cantabrian Region, Quat. Int., 433, 50–63, https://doi.org/10.1016/j.quaint.2016.02.020, 2017.

Rios-Garaizar, J., Arrizabalaga, A., and Villaluenga, A.: Haltes de chasse du Châtelperronien de la Péninsule Ibérique : Labeko Koba et Ekain (Pays Basque Péninsulaire), Anthropologie., 116, 532–549, https://doi.org/10.1016/j.anthro.2012.10.001, 2012.

Rios-Garaizar, J., de la Peña, P., and Maillo-Fernández, J. M.: El final del Auriñaciense y el comienzo del Gravetiense en la región cantábrica: una visión tecno-tipológica, in: Pensando El Gravetiense: Nuevos Datos Para La Región Cantábrica En Su Contexto Peninsular Y Pirenaico. Monografías Del Museo Nacional Y Centro de Investigación de Altamira, 23, edited by: de las Heras, C., Lasheras, J. A., Arrizabalaga, Á., and de la Rasilla, M., Ministerio de Educación, Cultura, Madrid, 369–382, 2013.

Rios-Garaizar, J., Iriarte, E., Arnold, L. J., Sánchez-Romero, L., Marín-Arroyo, A. B., San Emeterio, A., Gómez-Olivencia, A., Pérez-Garrido, C., Demuro, M., Campaña, I., Bourguignon, L., Benito-Calvo, A., Iriarte, M. J., Aranburu, A., Arranz-Otaegi, A., Garate, D., Silva-Gago, M., Lahaye, C., and Ortega, I.: The intrusive nature of the Châtelperronian in the Iberian Peninsula, PLoS One, 17, e0265219, 2022.

Rivals, F., Uzunidis, A., Sanz, M., and Daura, J.: Faunal dietary response to the Heinrich Event 4 in southwestern Europe, Palaeogeogr. Palaeoclim. Palaeoecol., 473, 123–130, https://doi.org/10.1016/j.palaeo.2017.02.033, 2017.

Sanz-Royo, A., Sanz, M., and Daura, J.: Upper Pleistocene equids from Terrasses de la Riera dels Canyars (NE Iberian Peninsula): The presence of Equus ferus and Equus hydruntinus based on dental criteria and their implications for palaeontological identification and palaeoenvironmental reconstr, Quat. Int., 566–567, 78–90, https://doi.org/10.1016/j.quaint.2020.06.026, 2020.

Sanz-Royo, A., Terlato, G., and Marín-Arroyo, A. B.: Taphonomic data from the transitional Aurignacian of El Castillo cave (Spain) reveals the role of carnivores at the Aurignacian Delta level, Quat. Sci. Adv., 13, 100147, https://doi.org/10.1016/j.qsa.2023.100147, 2024.

Vidal-Cordasco, M., Ocio, D., Hickler, T., and Marín-Arroyo, A. B.: Ecosystem productivity affected the spatiotemporal disappearance of Neanderthals in Iberia, Nat. Ecol. Evol., 6, 1644–1657, https://doi.org/10.1038/s41559-022-01861-5, 2022.

Villaluenga, A., Arrizabalaga, Á., and Rios-Garaizar, J.: Multidisciplinary approach to two Châtelperronian series: lower IX layer of Labeko Koba and X Level of Ekain (Basque country, Spain), J. Taphon., 10, 525–548, 2012.
Wood, R., Bernaldo de Quirós, F., Maíllo-Fernández, J. M., Tejero, J. M., Neira, A., and Higham, T.: El Castillo (Cantabria, northern Iberia) and the Transitional Aurignacian: Using radiocarbon dating to assess site taphonomy, Quat. Int., 474, 56–70, https://doi.org/10.1016/j.quaint.2016.03.005, 2018.
Wood, R. E., Arrizabalaga, A., Camps, M., Fallon, S., Iriarte-Chiapusso, M. J., Jones, R., Maroto, J., De la Rasilla, M., Santamaría, D., Soler, J., Soler, N., Villaluenga, A., and Higham, T. F. G.: The chronology of the earliest Upper Palaeolithic in northern Iberia: New insights from L'Arbreda, Labeko Koba and La Viña, J. Hum. Evol., 69, 91–109, https://doi.org/10.1016/j.jhevol.2013.12.017, 2014.
Yravedra, J. and Gómez-Castanedo, A.: Estudio zooarqueológico y tafonómico del yacimiento del Otero (Secadura, Voto, Cantabria), Espac. Tiempo y Forma. Ser. I, Nueva época. Prehist. y Arqueol., 3, 21–38, 2010.
Zilhao, J. and D'Errico, F.: The chronology of the Aurignacian and Transitional technocomplexes. Where do we stand?, in: The chronology of the Aurignacian and of the transitional technocomplexes Dating, stratigraphies, cultural implications. Proceedings of Symposium 61 of the XIVth Congress of the UISPP, 313–349, 2003.

Section S2 – Raw data

This material is directly available at https://github.com/ERC-Subsilience/Ungulate_enamel-carbonate and Zenodo (https://doi.org/10.5281/zenodo.13839189).

Section S3 – Individual Bayesian Models

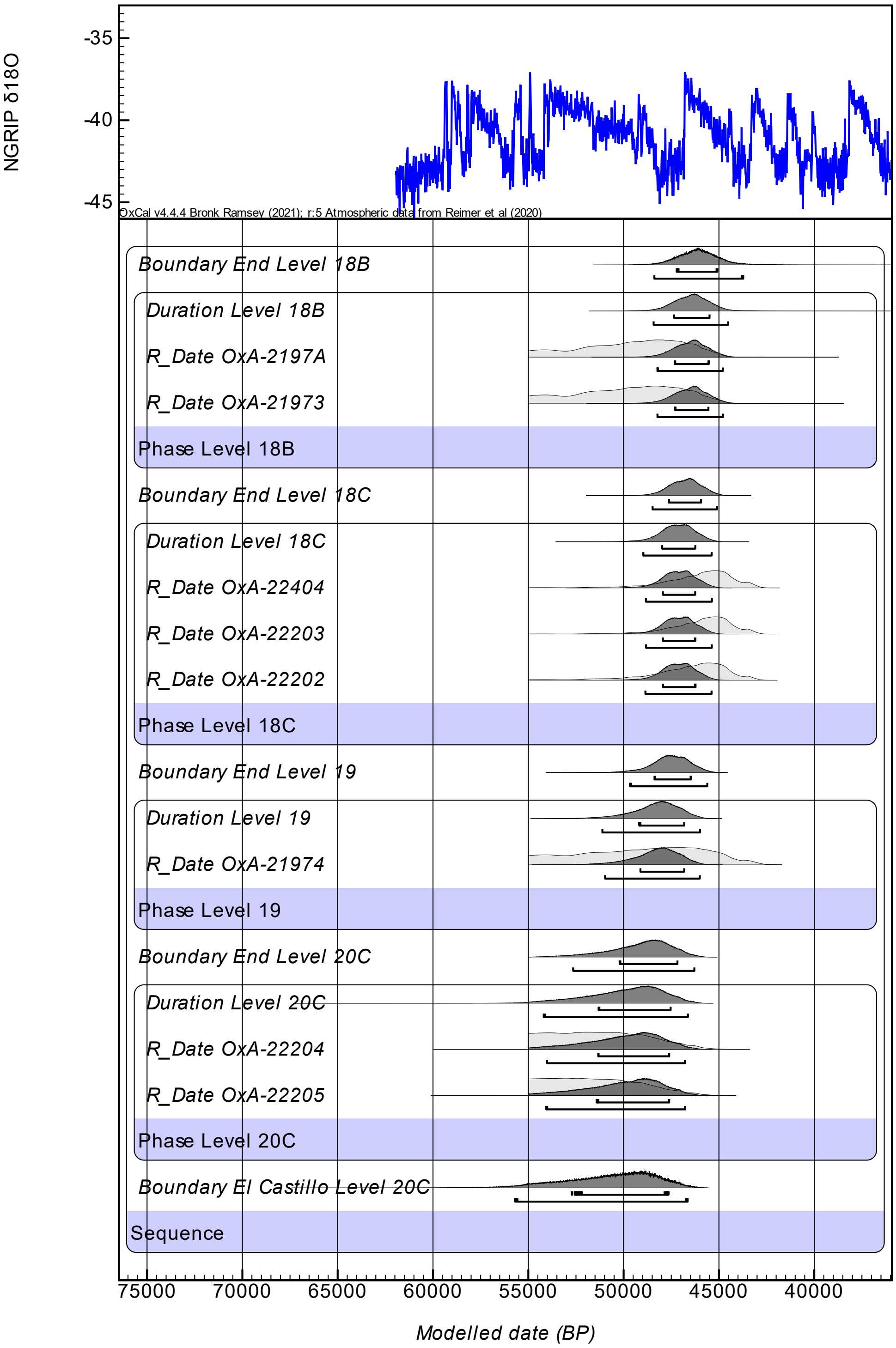

Figure S3.1. Radiocarbon dates from El Castillo modelled in OxCal4.4 against INTCAL20.

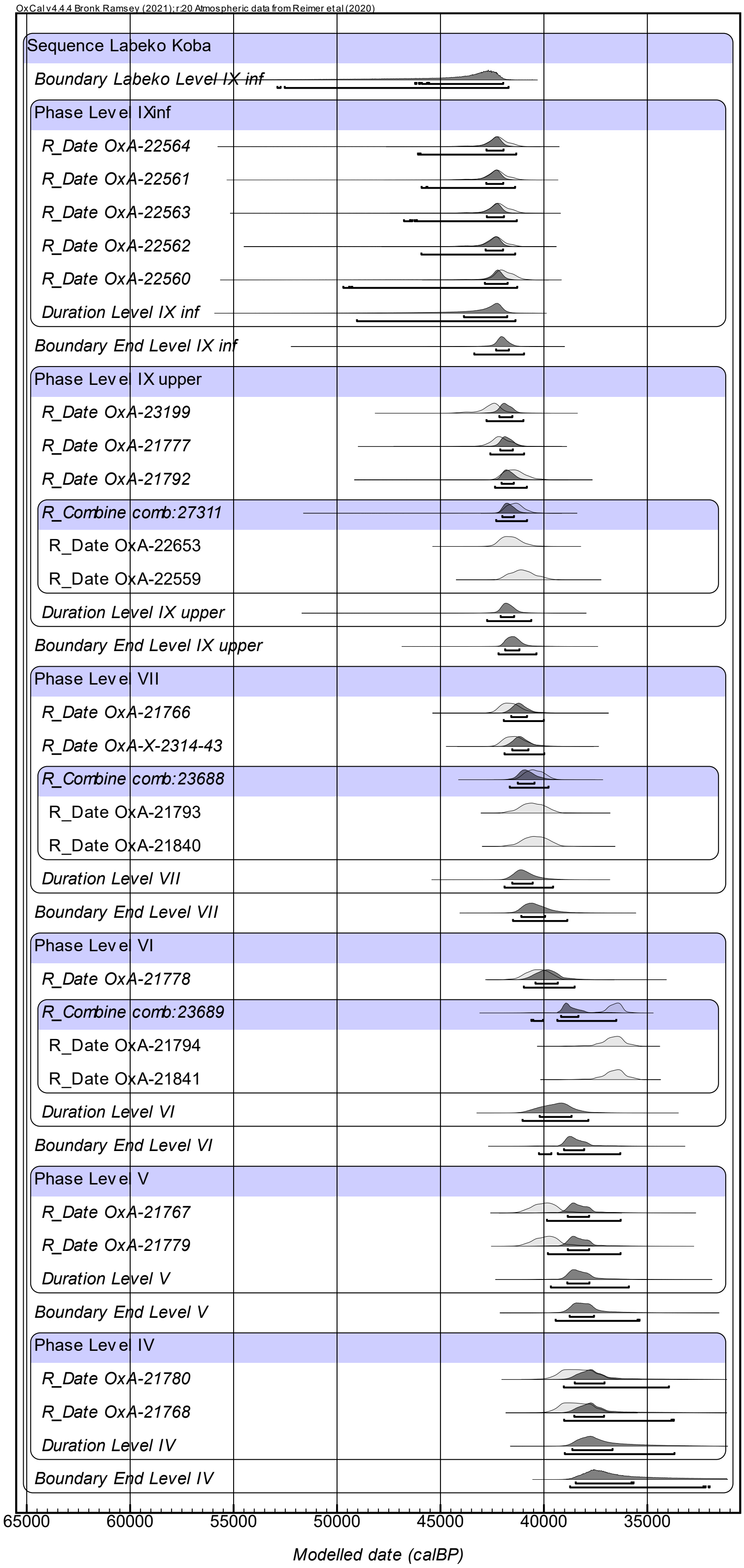

Figure S3.2. Radiocarbon dates from Labeko Koba modelled in OxCal4.4 against INTCAL20.

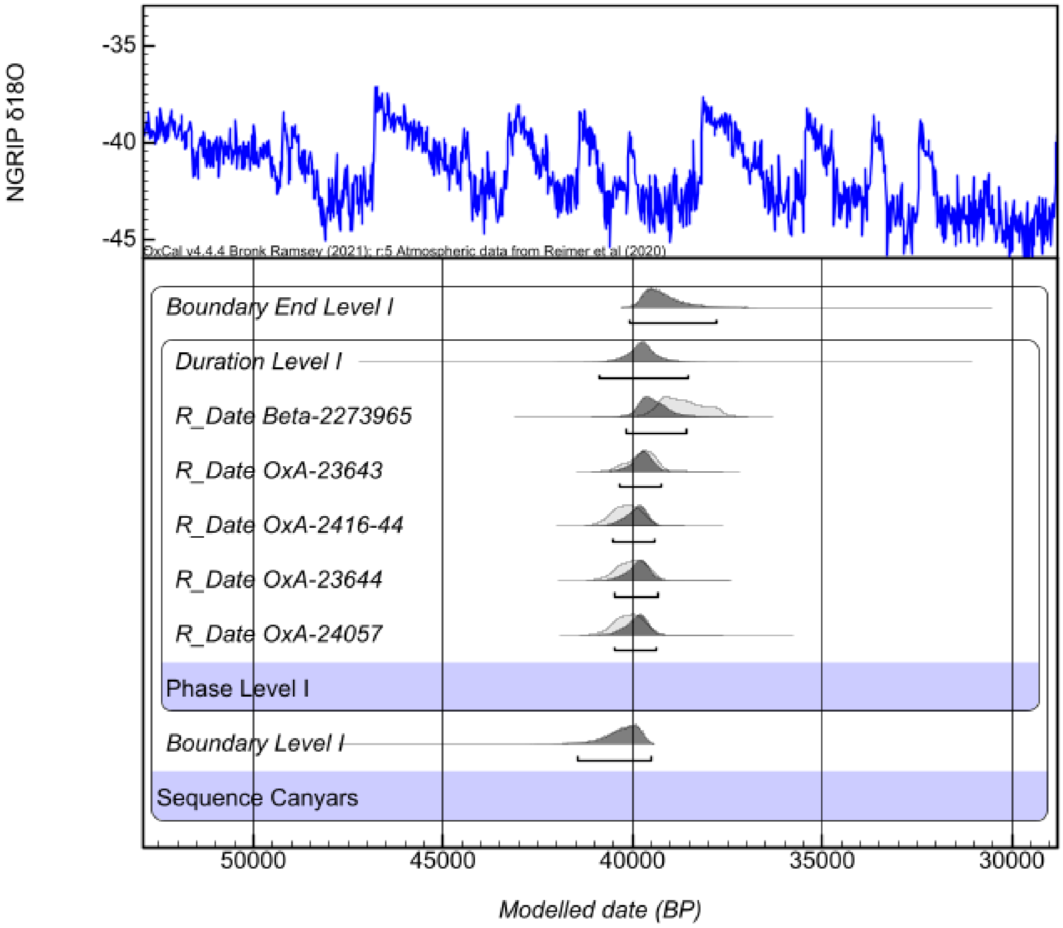

Figure S3.3. Radiocarbon dates from Canyars modelled in OxCal4.4 against INTCAL20.

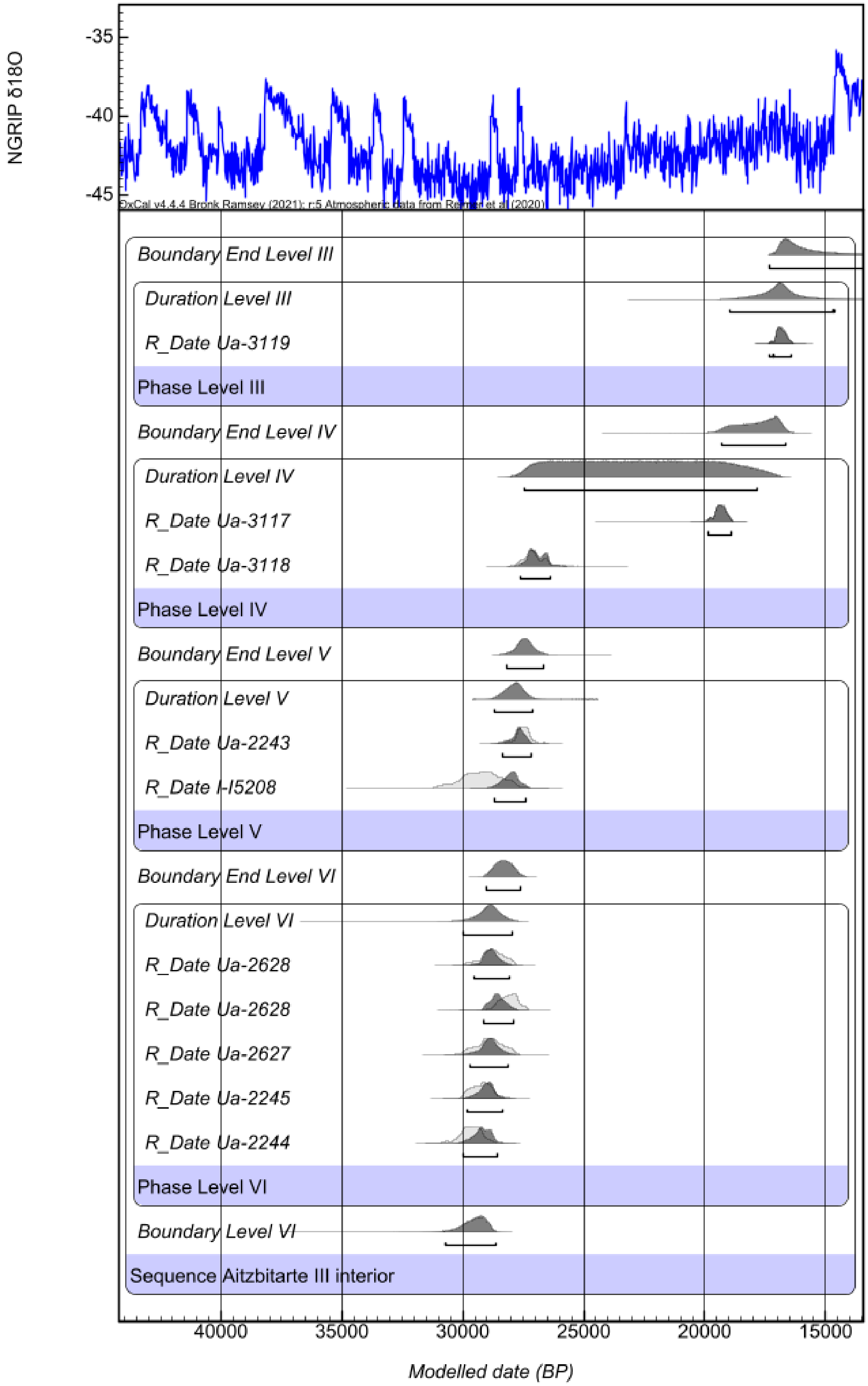

382

383 **Figure S3.4.** Radiocarbon dates from Aitzbitarte III-interior modelled in OxCal4.4 against INTCAL20.

Section 3 – Results of Bayesian Models

El Castillo	Unmodelled (BP)			Modelled (BP)			Indices Amodel 78.8, Aoverall 82.4			
	from	to	%	from	to	%	A	L	P	C
Boundary End Level 18B				48383	43733	95.449.974				97.1
Duration Level 18B				**48438**	**44536**	**95.449.974**				**99.8**
R_Date OxA-2197A	...	45427	95.449.973	48235	44793	95.449.974	98.1		95.2	99.8
R_Date OxA-21973	...	45655	95.449.973	48240	44793	95.449.974	91.9		95.2	99.8
Phase Level 18B										
Boundary End Level 18C				48470	45117	95.449.974				99.8
Duration Level 18C				**48977**	**45382**	**95.449.974**				**99.9**
R_Date OxA-22404	49976	42918	95.449.974	48833	45383	95.449.974	82.2		95.3	99.8
R_Date OxA-22203	49451	42999	95.449.974	48819	45381	95.449.974	76.1		95.2	99.8
R_Date OxA-22202	51146	43039	95.449.974	48861	45386	95.449.974	101.2		95.4	99.8
Phase Level 18C										
Boundary End Level 19				49629	45623	95.449.974				99.7
Duration Level 19				51060	45997	95.449.974				99.7
R_Date OxA-21974	...	44367	95.449.974	50965	45998	95.449.974	120.2		95.3	99.8
Phase Level 19										
Boundary End Level 20C				52583	46286	95.449.974				99.5
Duration Level 20C				**54134**	**46593**	**95.449.974**				**99.3**
R_Date OxA-22204	...	47048	95.449.974	53958	46713	95.449.974	94		95.3	99.3
R_Date OxA-22205	...	47348	95.449.974	53965	46715	95.449.974	86.9		95.3	99.3
Phase Level 20C										
Boundary El Castillo Level 20C				55552	46609	95.449.974				95.3
Sequence										
U(0	68.268.949	3.99E-17	4	68.268.949	5.38E-17	3.776		100		
T(5)	-2.65	2.65	95.449.974							99.9
Outlier_Model General				-2684	2502	95.449.974				100

Table S3.1. Radiocarbon dates from El Castillo modelled in OxCal4.4 against INTCAL20.

Aitzbitarte III Interior	Unmodelled (BP)			Modelled (BP)			Indices Amodel 78.8, Aoverall 82.4			
	from	to	%	from	to	%	A	L	P	C
Boundary End Level III				17300	12910	9.544.997				98
Duration Level III				18960	14630	9.544.997				99.6
R_Date Ua-3119	17270	16390	9.544.997	17300	16430	9.544.997	100.8		95.8	99.8
Phase Level III										
Boundary End Level IV				19320	16640	9.544.997				99.3
Duration Level IV				27430	17820	9.544.997				98.9
R_Date Ua-3117	19830	18900	9.544.997	19840	18910	9.544.997	99.9		95.3	99.6
R_Date Ua-3118	27700	26430	9.544.997	27600	26360	9.544.997	98.1		95.2	99.5
Phase Level IV										
Boundary End Level V				28210	26680	9.544.997				99.7
Duration Level V				**28680**	**27130**	**9.544.997**				**99.9**
R_Date Ua-2243	28260	26610	9.544.997	28370	27190	9.544.997	88.8		95.4	99.8
R_Date I-I5208	30830	27760	9.544.997	28710	27370	9.544.997	57.7		94.8	99.8
Phase Level V										
Boundary End Level VI				29010	27630	9.544.997				99.7
Duration Level VI				29990	27930	9.544.997				99.8
R_Date Ua-2628	29760	27840	9.544.997	29570	28080	9.544.997	118.2		96	99.8
R_Date Ua-2628	28760	27360	9.544.997	29150	27920	9.544.997	67		94.3	99.8
R_Date Ua-2627	29920	27870	9.544.997	29680	28110	9.544.997	120.5		96	99.8
R_Date Ua-2245	30070	28280	9.544.997	29820	28360	9.544.997	108		95.9	99.8
R_Date Ua-2244	30720	28760	9.544.997	30010	28570	9.544.997	77.7		94.9	99.7
Phase Level VI										
Boundary Level VI				30730	28650	9.544.997				96
Sequence										
U(0,4)	3.99E-17	4	9.544.997	5.38E-17	3.772	9.544.997	100			99
T(5)	-2.65	2.65	9.544.997							95.5
Outlier_Model General				-1420	1280	9.544.997				99.9

Table S3.2. Radiocarbon dates from Labeko Koba modelled in OxCal4.4 against INTCAL20.

Canyars	Unmodelled (BP)			Modelled (BP)			Indices Amodel 78.8, Aoverall 82.4			
Boundary End Level I				40090	37770	95.45				95.3
Duration Level I				**40890**	**38530**	**95.45**				**99.7**
R_Date Beta-2273965	39630	37570	9.544.997	40190	38560	95.45	63.2		93.4	99.6
R_Date OxA-23643	40520	39140	9.544.997	40330	39240	95.45	114.2		96.1	99.8
R_Date OxA-2416-44	40880	39450	9.544.997	40540	39400	95.45	99.2		96	99.8
R_Date OxA-23644	40740	39300	9.544.997	40470	39340	95.45	110.5		96	99.8
R_Date OxA-24057	40790	39390	9.544.997	40490	39380	95.45	104.3		96	99.8
Phase Level I										
Boundary Level I				41450	39500	95.45				96.6
Sequence Canyars										
U(0,4)	3.99E-17	4	9.544.997	5.38E-17	3.82	95.45	100			100
T(5)	-2.65	2.65	9.544.997							99.4
Outlier_Model General				-800	1480	95.45				99.9

Table S3.3. Radiocarbon dates from Canyars modelled in OxCal4.4 against INTCAL20.

Labeko Koba	Unmodelled (BP)			Modelled (BP)			Indices Amodel 78.8, Aoverall 82.4			
	from	to	%	from	to	%	A	L	P	C
Boundary End Level IV				38710	32030	9.544.997				98.4
Duration Level IV				**39000**	**33710**	**9.544.997**				**99.8**
R_Date OxA-21768	39700	37030	9.544.997	39050	33820	9.544.997	75.5		80	99.8
R_Date OxA-21780	39780	36910	9.544.997	39050	33960	9.544.997	81.3		82.3	99.8
Phase Level IV										
Boundary End Level V				39470	35440	9.544.997				99.8
Duration Level V				**39730**	**35950**	**9.544.997**				**99.8**
R_Date OxA-21779	41170	38260	9.544.997	39830	36330	9.544.997	21		87.2	99.8
R_Date OxA-21767	41230	38500	9.544.997	39860	36340	9.544.997	15.5		85.5	99.8
Phase Level V										
Boundary End Level VI				40240	36360	9.544.997				99.8
Duration Level VI				**41030**	**37860**	**9.544.997**				**99.9**
R_Date OxA-21841	37710	35420	9.544.997							
R_Date OxA-21794	38040	35460	9.544.997							
R_Combine comb:23689	37350	35900	9.544.997	40620	36500	9.544.997	4.3			99.8
R_Date OxA-21778	41390	39190	9.544.997	40970	38550	9.544.997	90		94.4	99.9
Phase Level VI										
Boundary End Level VII				41490	38890	9.544.997				99.9
Duration Level VII				**41910**	**39570**	**9.544.997**				**99.9**
R_Date OxA-21840	41610	39250	9.544.997							
R_Date OxA-21793	41720	39390	9.544.997							
R_Combine comb:23688	41290	39570	9.544.997	41650	39780	9.544.997	87.3			99.9
R_Date OxA-X-2314-43	42350	40260	9.544.997	41900	40000	9.544.997	96.5		95.4	99.9
R_Date OxA-21766	42520	40530	9.544.997	41950	40020	9.544.997	80.3		94.6	99.9
Phase Level VII										
Boundary End Level IX upper				42190	40360	9.544.997				99.9
Duration Level IX upper				**42750**	**40580**	**9.544.997**				**99.9**
R_Date OxA-22559	42090	39850	9.544.997							
R_Date OxA-22653	42520	40530	9.544.997							
R_Combine comb:27311	42120	40600	9.544.997	42330	40800	9.544.997	95			99.9
R_Date OxA-21792	42370	40330	9.544.997	42380	40820	9.544.997	113.4		95.7	99.9
R_Date OxA-21777	43160	40960	9.544.997	42600	40950	9.544.997	99.5		95.6	99.9
R_Date OxA-23199	43980	41490	9.544.997	42800	40990	9.544.997	52.4		92.8	99.9
Phase Level IX upper										
Boundary End Level IX inf				43420	40970	9.544.997				99.9
Duration Level IX inf				**48940**	**41340**	**9.544.997**				**99.8**
R_Date OxA-22560	42780	40980	9.544.997	49670	41300	9.544.997	75.3		76	99.8
R_Date OxA-22562	43830	41220	9.544.997	45860	41380	9.544.997	102.8		90.9	99.8
R_Date OxA-22563	43250	41010	9.544.997	46280	41300	9.544.997	99.1		89.7	99.8
R_Date OxA-22561	43790	41130	9.544.997	45920	41340	9.544.997	102.3		90.7	99.8
R_Date OxA-22564	43370	41050	9.544.997	46060	41320	9.544.997	101		90.2	99.8
Phase Level IXinf										
Boundary Labeko Level IX inf				52660	41740	9.544.997				96.6
Sequence Labeko Koba										
N(0,2)	-4	4	9.544.997							99.4
Outlier_Model SSimple				...	840	9.544.997				97.5
U(0,4)	3.99E-17	4	9.544.997	5.38E-17	3.932	9.544.997	100			98.3
T(5)	-2.65	2.65	9.544.997							97.5
Outlier_Model General				-6130	9280	9.544.997				99.4

Table S3.4. Radiocarbon dates from Aitzbitarte III-interior modelled in OxCal4.4 against INTCAL20.

Section 4 – Intra-tooth curve plots

Original curves derived from enamel intra-tooth sampling on enamel carbonate provided by sites. In blue, oxygen stable isotope composition ($\delta^{18}O$), and, in brown, carbon stable isotope composition ($\delta^{13}C$). In the x-axis, the distance from the Enamel Rooth Junction (ERJ). Notice that the y-axis can experience some variations between sites.

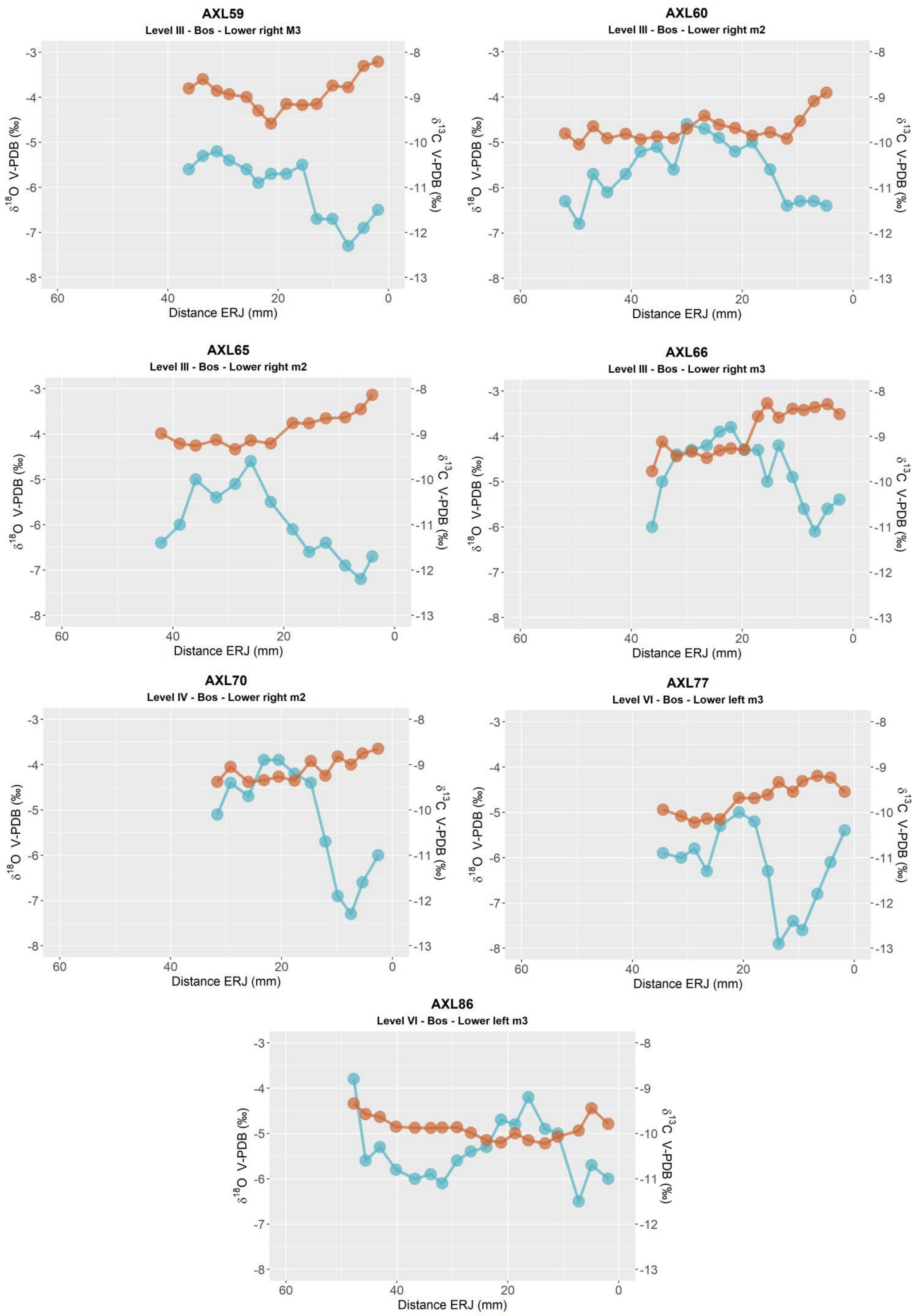

Figure S4.1. Intra-tooth plots of oxygen ($\delta^{18}O$) and carbon ($\delta^{13}C$) isotope composition from teeth from Axlor, considering distance from enamel root junction (ERC).

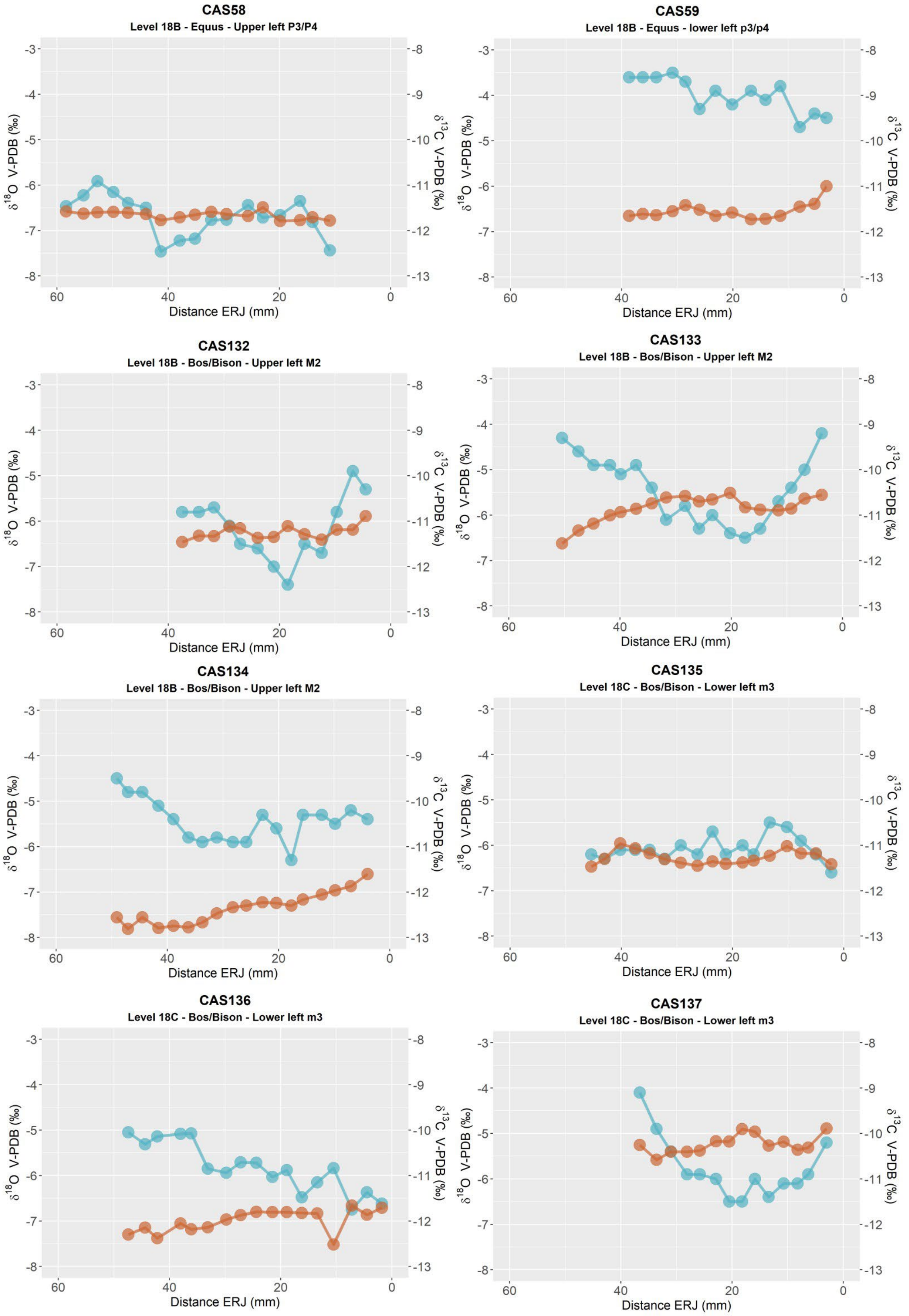

Figure S4.2. Intra-tooth plots of oxygen ($\delta^{18}O$) and carbon ($\delta^{13}C$) isotope composition from teeth from El Castillo, considering the sample's distance from the enamel root junction (ERC).

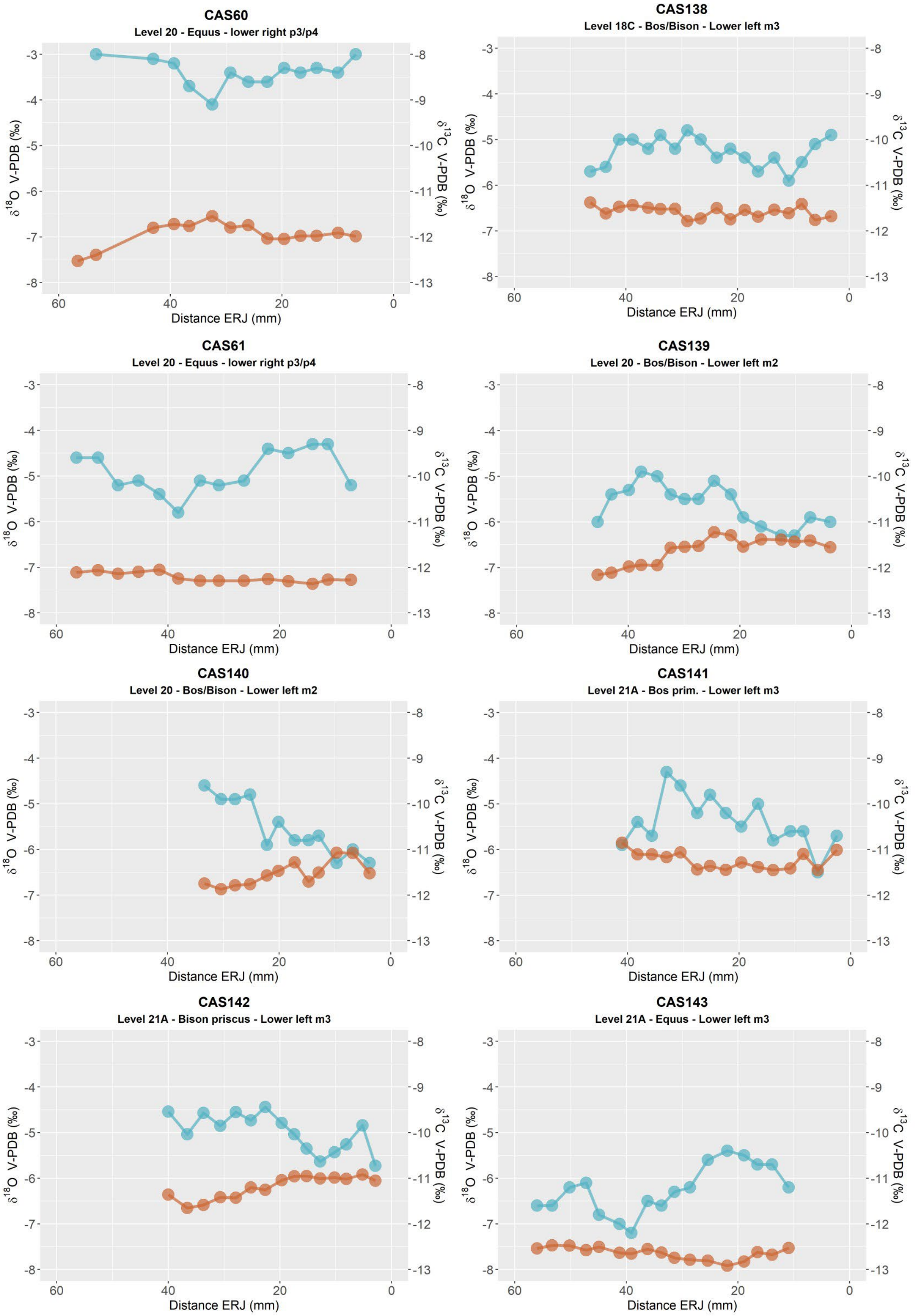
CAS60
Level 20 - Equus - lower right p3/p4
CAS138
Level 18C - Bos/Bison - Lower left m3
CAS61
Level 20 - Equus - lower right p3/p4
CAS139
Level 20 - Bos/Bison - Lower left m2
CAS140
Level 20 - Bos/Bison - Lower left m2
CAS141
Level 21A - Bos prim. - Lower left m3
CAS142
Level 21A - Bison priscus - Lower left m3
CAS143
Level 21A - Equus - Lower left m3
δ18O V-PDB (‰)
δ13C V-PDB (‰)
Distance ERJ (mm)

Figure S4.3. Intra-tooth plots of oxygen ($\delta^{18}O$) and carbon ($\delta^{13}C$) isotope composition from teeth from El Castillo, considering the sample's distance from the enamel root junction (ERC).

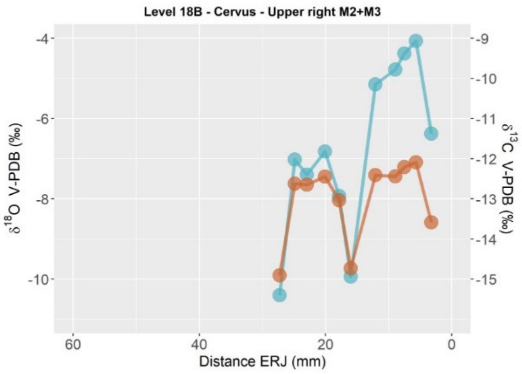

Figure S4.4. Intra-tooth plots of oxygen ($\delta^{18}O$) and carbon ($\delta^{13}C$) isotope composition from teeth from El Castillo, considering the sample's distance from the enamel root junction (ERC).

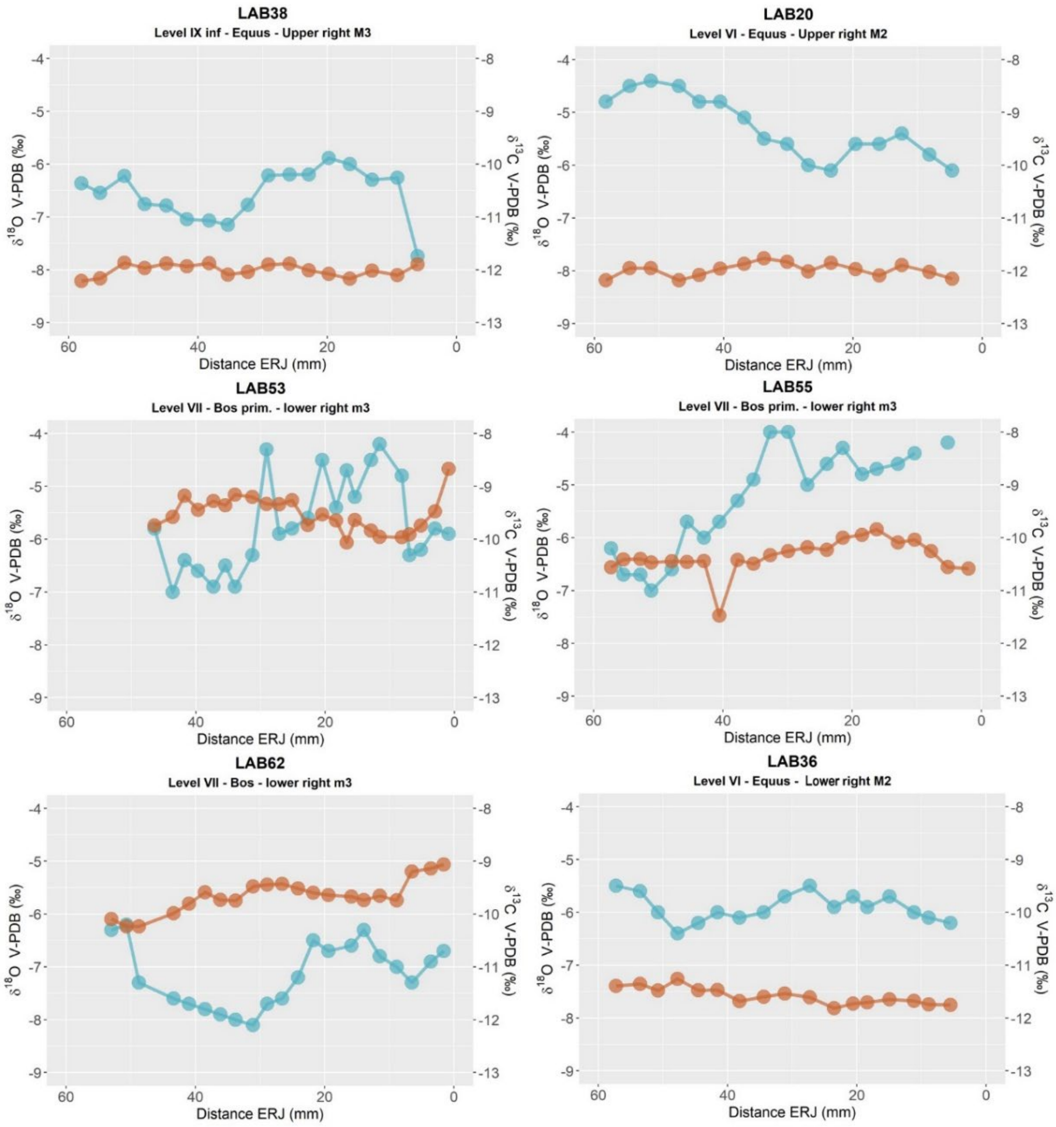

Figure S4.5. Intra-tooth plots of oxygen ($\delta^{18}O$) and carbon ($\delta^{13}C$) isotope composition from teeth from Labeko Koba, considering the sample's distance from the enamel root junction (ERC).

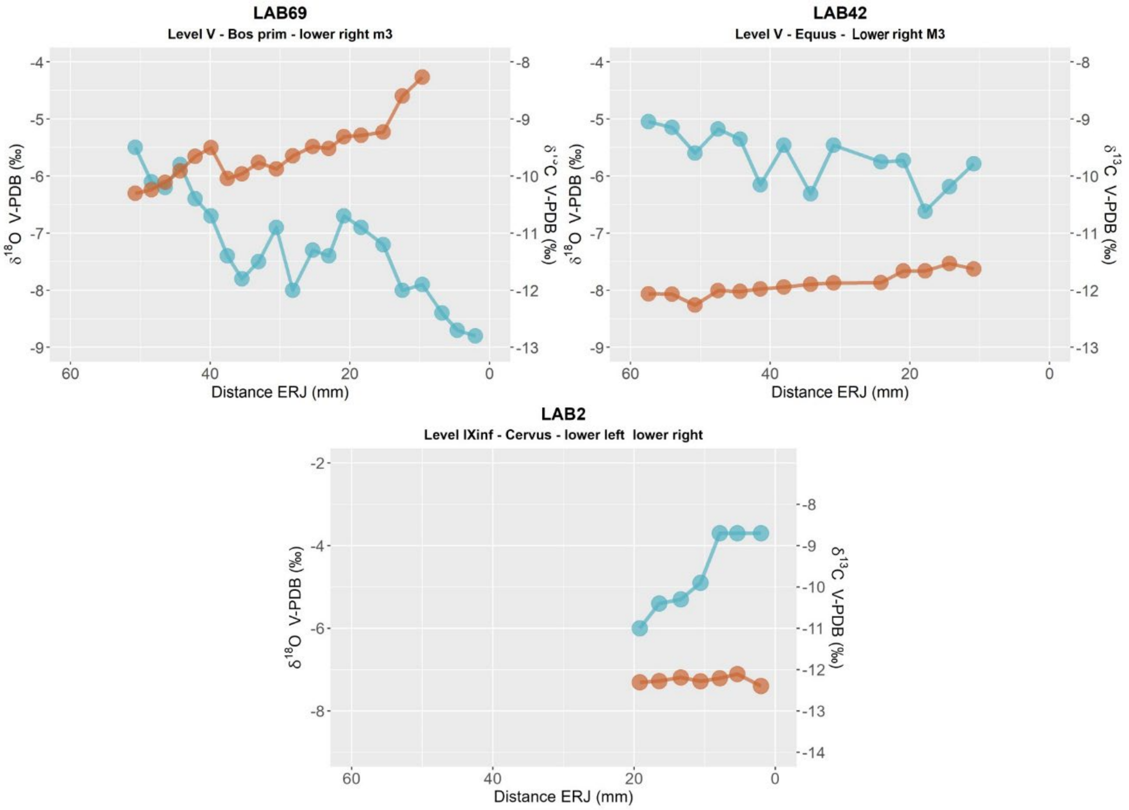

Figure S4.6. Intra-tooth plots of oxygen ($\delta^{18}O$) and carbon ($\delta^{13}C$) isotope composition from teeth from Labeko Koba, considering the sample's distance from the enamel root junction (ERC).

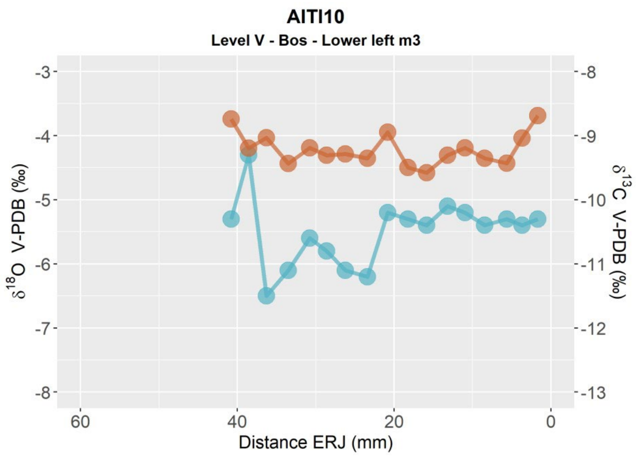

Figure S4.7. Intra-tooth plots of oxygen ($\delta^{18}O$) and carbon ($\delta^{13}C$) isotope composition from teeth from Aitzbitarte III interior, considering the sample's distance from the enamel root junction (ERC).

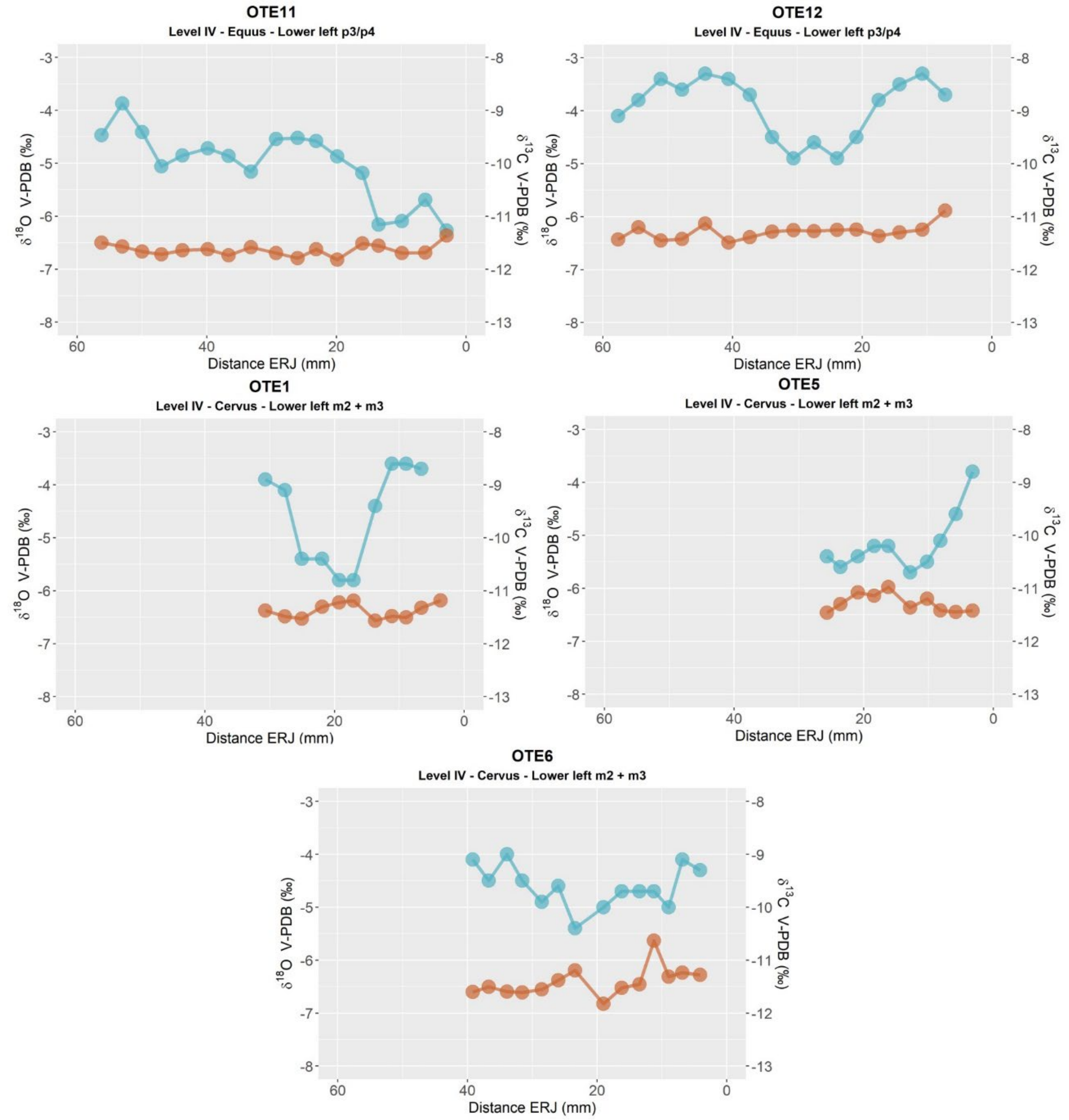

Figure S4.8. Intra-tooth plots of oxygen ($\delta^{18}O$) and carbon ($\delta^{13}C$) isotope composition from teeth from El Otero, considering the sample's distance from the enamel root junction (ERC).

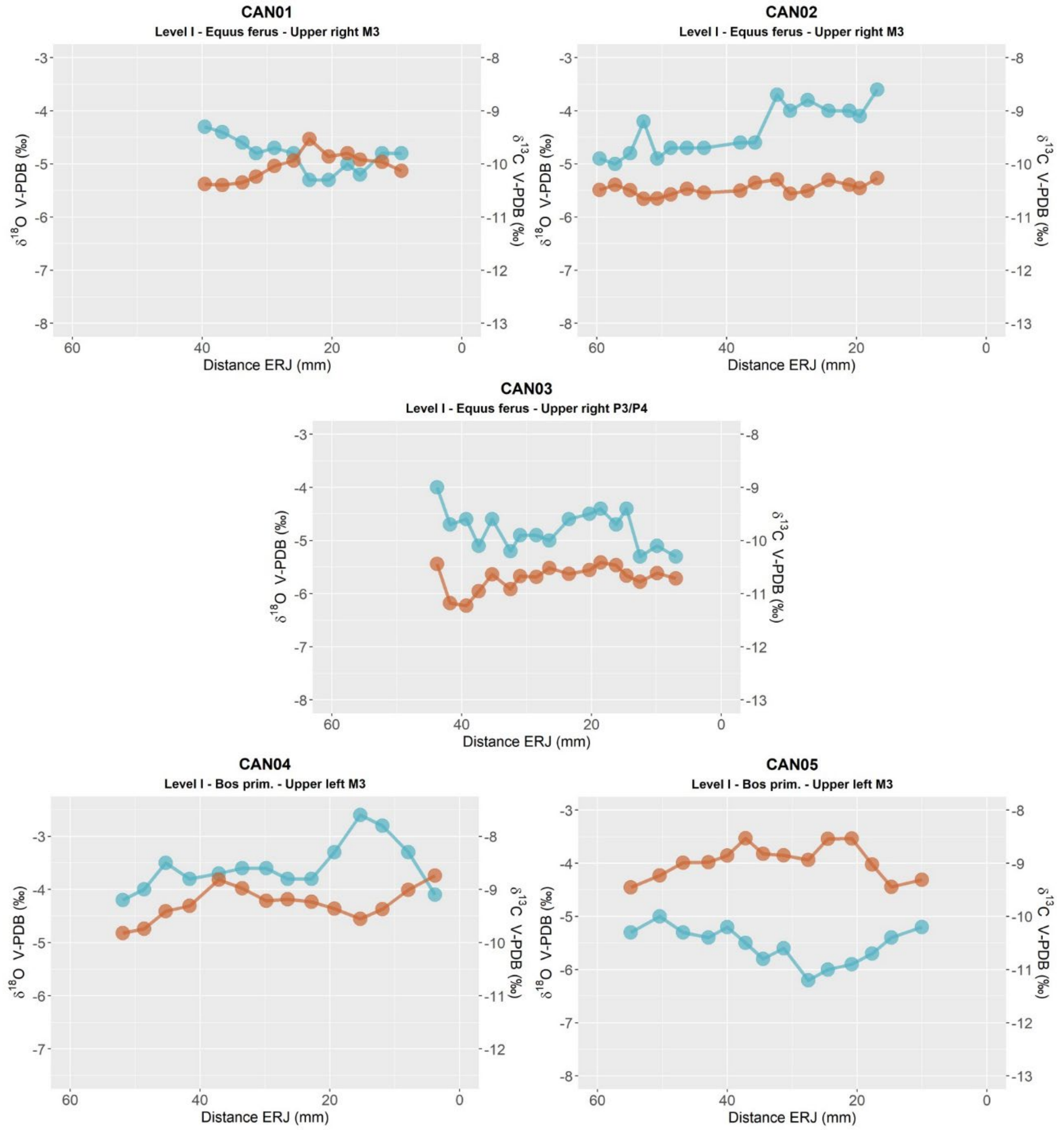

Figure S4.9. Intra-tooth plots of oxygen ($\delta^{18}O$) and carbon ($\delta^{13}C$) isotope composition from teeth from Canyars considering the sample's distance from the enamel root junction (ERC).

Section 5 – Inverse Modelling: Methodological Details and Models

The intra-tooth $\delta^{18}O$ profiles presented in this study were obtained through the application of inverse modelling, using an adapted version of the code published in reference (Passey et al., 2005b). This modeling approach allowed for the correction of the damping effect and the reconstruction of the original $\delta^{18}O$ input time series. The model reproduces the temporal delay between $\delta^{18}O$ changes in the animal's input and their manifestation in tooth enamel, exhibiting a consistent x-direction delay in the modelled $\delta^{18}O$ curve relative to the enamel $\delta^{18}O$ input time series. The model utilizes different species-specific parameters related to enamel formation, which vary between bovines and equids. These parameters have been established based on previous studies (Bendrey et al., 2015; Zazzo et al., 2012; Passey and Cerling, 2002; Kohn, 2004; Blumenthal et al., 2014). For *Bos/Bison* sp., the initial mineral content of enamel is fixed at 25%, the enamel appositional length is set at 1.5 mm, and the maturation length is 25 mm. For *Equus* sp., the initial mineral content of enamel is fixed at 22%, the enamel appositional length is set at 6 mm, and the maturation length is 28 mm.

In addition, the model requires other variables related to sampling geometry, as well as error estimates derived from mass spectrometer measurements. The distance between samples varies for each tooth, but as a general trend, the sampling depth on the tooth enamel surface in the samples of this study represents approximately 70% of the total enamel depth. The standard deviation of the measurements obtained from the mass spectrometer was typically set at 0.12%, taking into account the uncertainty associated with the standards. Finally, the models require a damping factor that determines the cumulative damping along the isotopic profile by adjusting the measured error (Emeas) to the prediction error (Epred). In the teeth analysed in this study, the damping factor ranged from 0.001 to 0.1.

The most likely model solutions were selected, and summer and winter values were extracted from the $\delta^{18}O$ profiles, considering the original peaks and troughs identified in the unmodelled $\delta^{18}O$ profile. This approach was adopted to prevent the introduction of artificial peaks that the model may produce, particularly in teeth without a distinct sinusoidal shape. Flat and less sinusoidal profile are less suitable for the application of the model, given its inherent assumption of an approximately sinusoidal form. Non-sinusoidal curves can lead to complex interpretations in the model outcomes. Consequently, this methodology was not applied to analysed intra-tooth $\delta^{13}C$ profiles, as the examined individuals did not exhibit appreciable seasonal change.

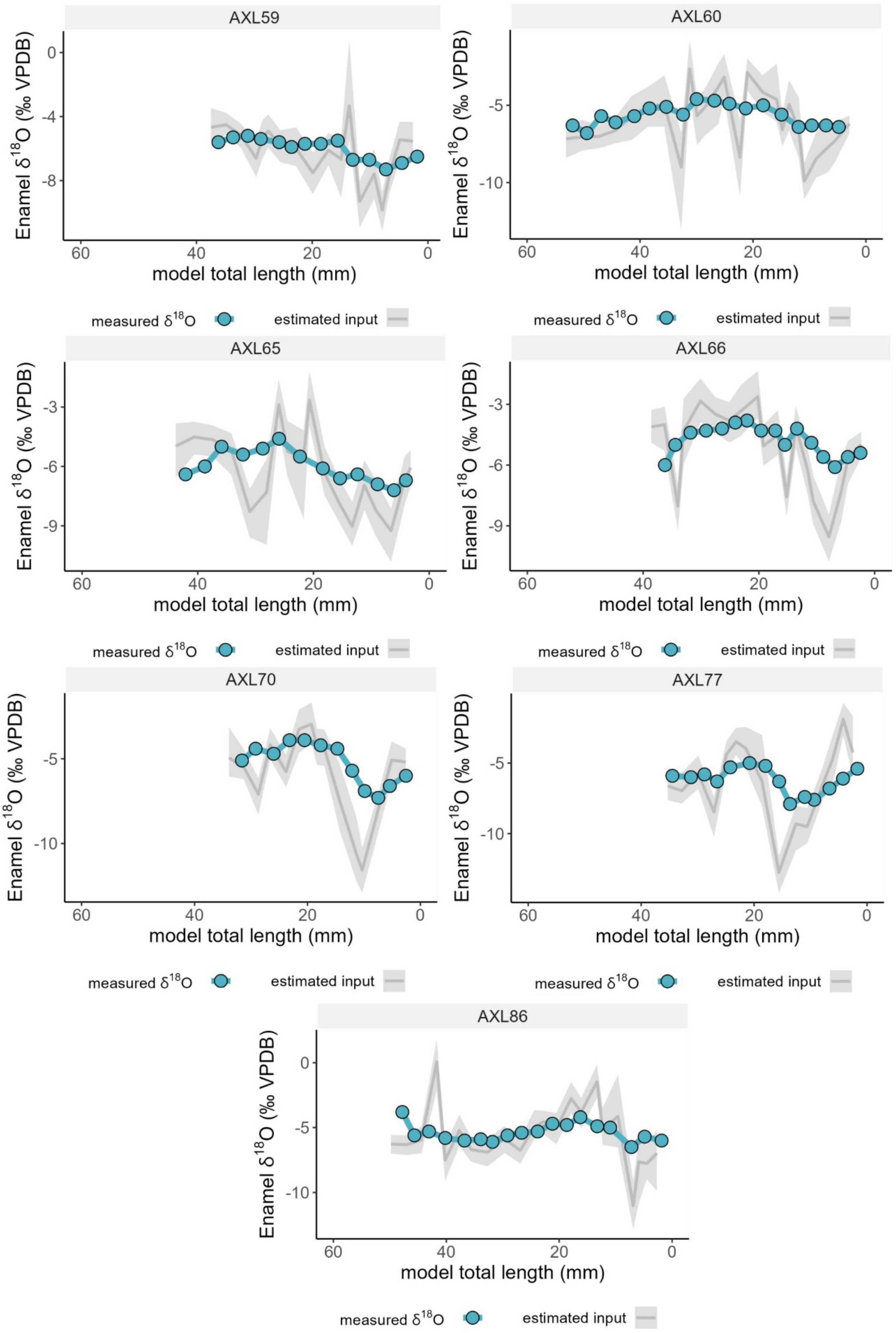

Figure S5.1. Inverse models for oxygen isotope composition ($\delta^{18}O$) from teeth from Axlor, considering distance from enamel root junction. The blue line and points correspond to original data and grey line the most likely model solution, with the 95% confidence interval shown in shaded areas.

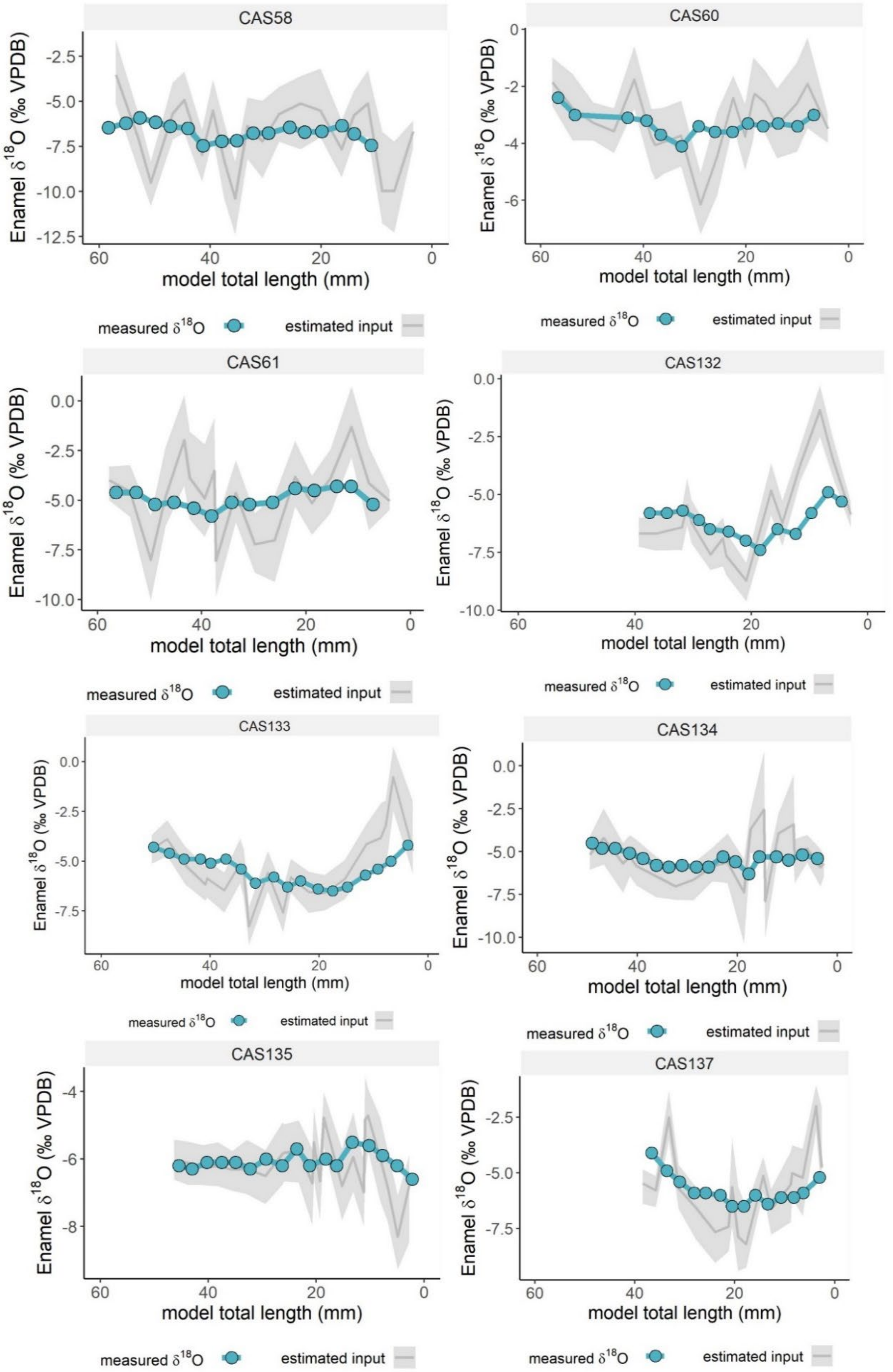

Figure S5.2. Inverse models for oxygen isotope composition ($\delta^{18}O$) from teeth from El Castillo, considering distance from enamel root junction. The blue line and points correspond to original data and grey line the most likely model solution, with the 95% confidence interval shown in shaded areas.

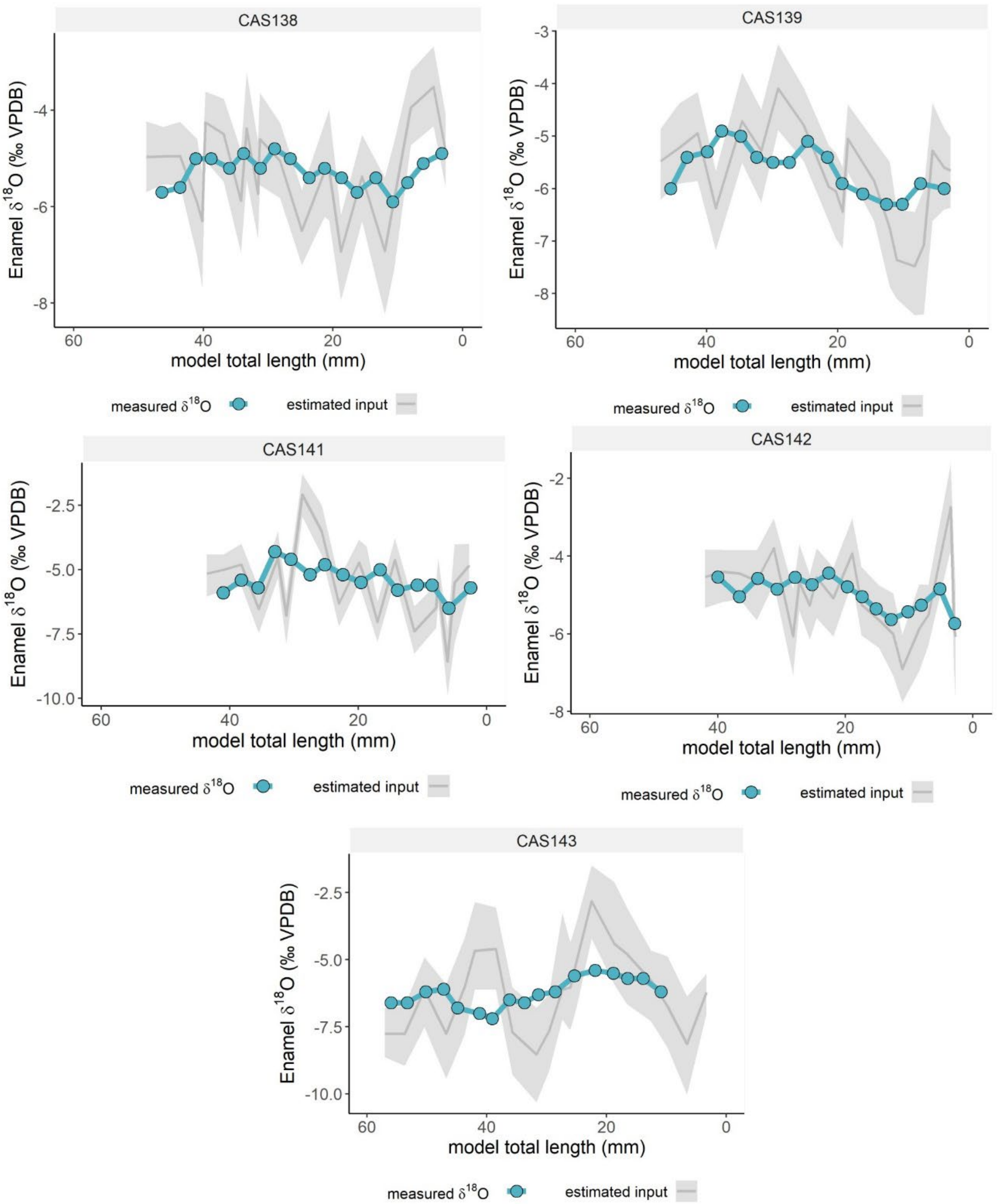

Figure S5.3. Inverse models for oxygen isotope composition ($\delta^{18}O$) from teeth from El Castillo, considering distance from enamel root junction. The blue line and points correspond to the original data and the grey line is the most likely model solution, with the 95% confidence interval shown in shaded areas.

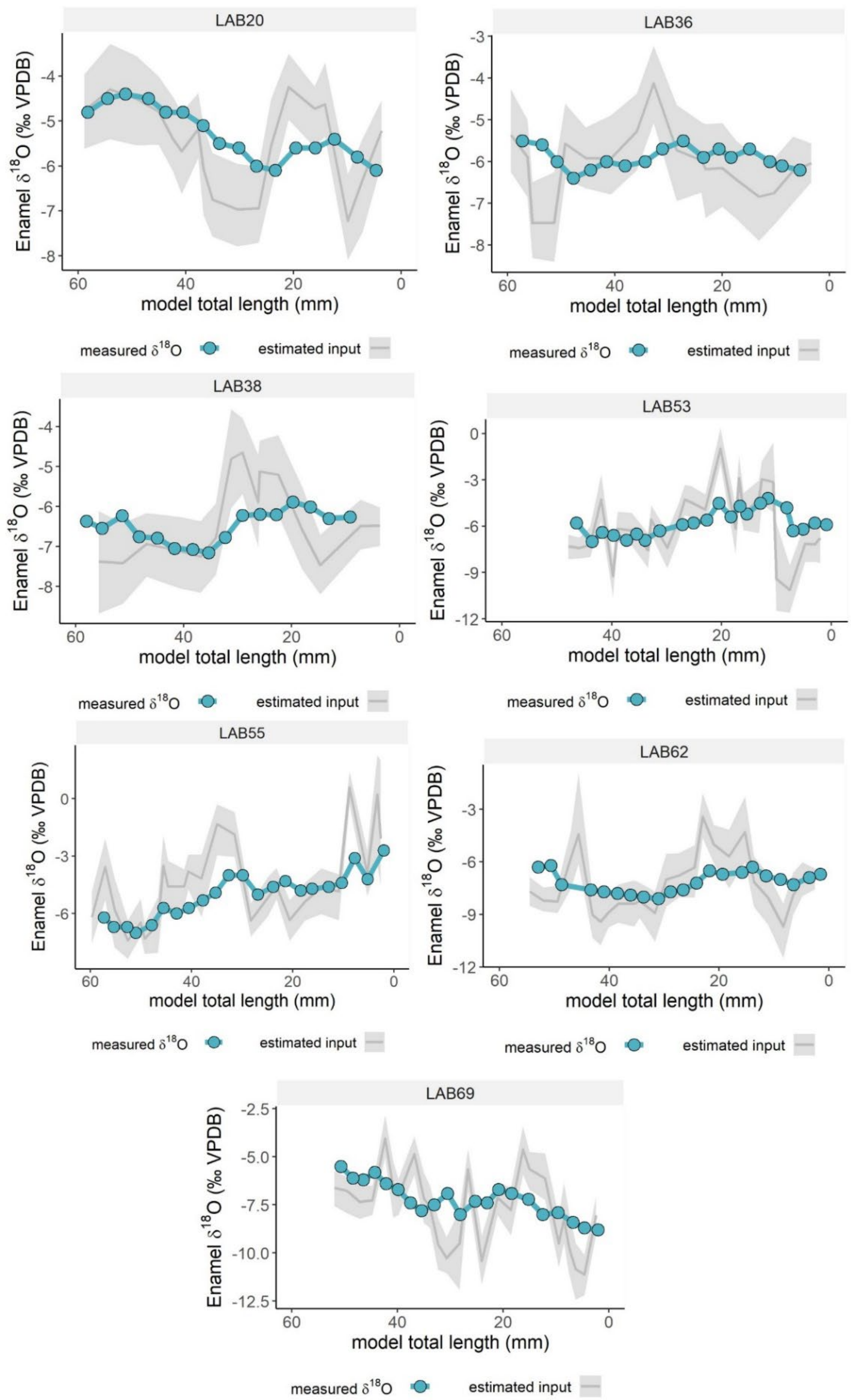

Figure S5.4. Inverse models for oxygen isotope composition ($\delta^{18}O$) from teeth from Labeko Koba, considering distance from enamel root junction. The blue line and points correspond to the original data, and the grey line is the most likely model solution, with the 95% confidence interval shown in shaded areas.

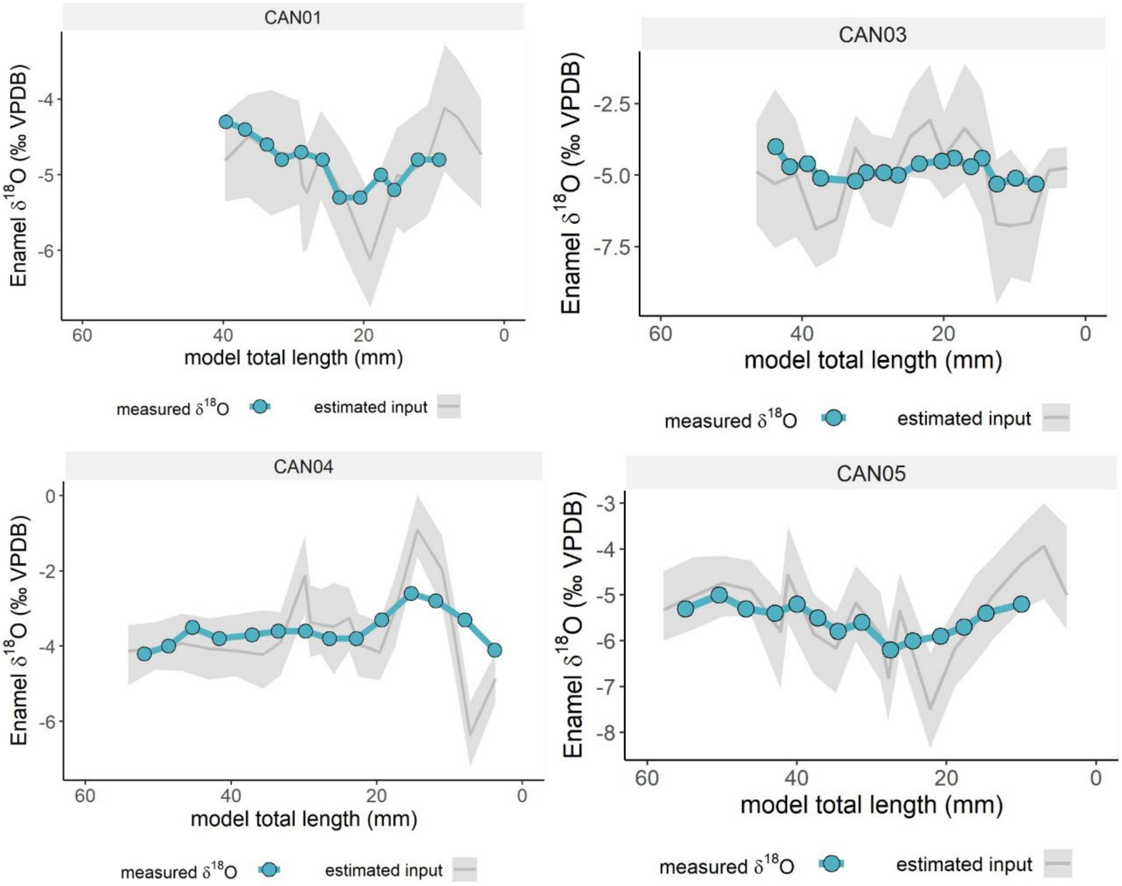

Figure S5.5. Inverse models for oxygen isotope composition (δ^{18}O) from teeth from Canyars considering distance from enamel root junction. The blue line and points correspond to original data and grey line the most likely model solution, with the 95% confidence interval shown in shaded areas.

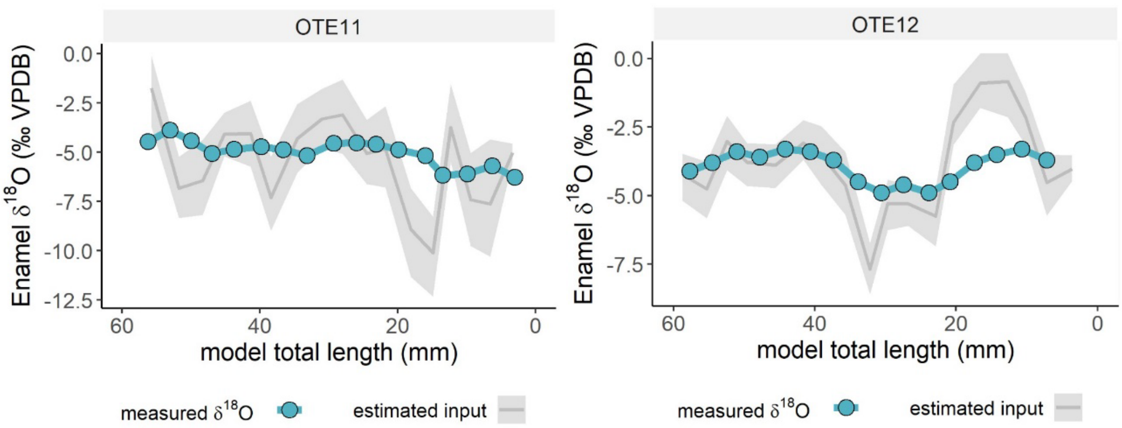

Figure S5.6. Inverse models for oxygen isotope composition (δ^{18}O) from teeth from El Otero, considering distance from enamel root junction. The blue line and points correspond to original data and the grey line is the most likely model solution, with the 95% confidence interval shown in shaded areas.

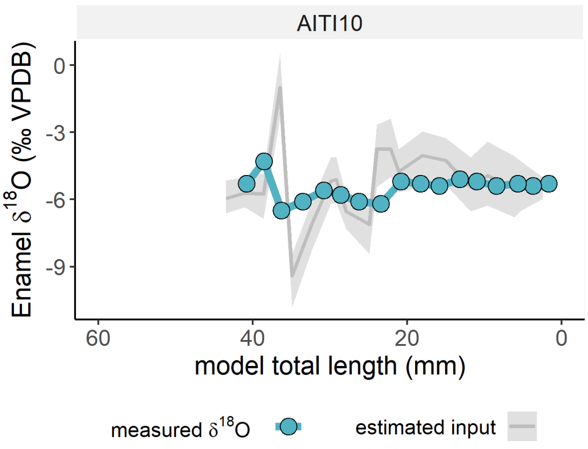

Figure S5.7. Inverse models for oxygen isotope composition ($\delta^{18}O$) from teeth from Aitzbitarte III interior, considering distance from enamel root junction. The blue line and points correspond to the original data, and the grey line is the most likely model solution, with the 95% confidence interval shown in shaded areas.

References Section 5

Bendrey, R., Vella, D., Zazzo, A., Balasse, M., and Lepetz, S.: Exponentially decreasing tooth growth rate in horse teeth: implications for isotopic analyses, Archaeometry, 57, 1104–1124, https://doi.org/10.1111/arcm.12151, 2015.

Blumenthal, S. A., Cerling, T. E., Chritz, K. L., Bromage, T. G., Kozdon, R., and Valley, J. W.: Stable isotope time-series in mammalian teeth: In situ δ18O from the innermost enamel layer, Geochim. Cosmochim. Acta, 124, 223–236, https://doi.org/10.1016/j.gca.2013.09.032, 2014.

Kohn, M. J.: Comment: Tooth Enamel Mineralization in Ungulates: Implications for Recovering a Primary Isotopic Time-Series, by B. H. Passey and T. E. Cerling (2002), Geochim. Cosmochim. Acta, 68, 403–405, https://doi.org/10.1016/S0016-7037(03)00443-5, 2004.

Passey, B. H. and Cerling, T. E.: Tooth enamel mineralization in ungulates: implications for recovering a primary isotopic time-series, Geochim. Cosmochim. Acta, 66, 3225–3234, https://doi.org/10.1016/S0016-7037(02)00933-X, 2002.

Passey, B. H., Robinson, T. F., Ayliffe, L. K., Cerling, T. E., Sponheimer, M., Dearing, M. D., Roeder, B. L., and Ehleringer, J. R.: Carbon isotope fractionation between diet, breath CO2, and bioapatite in different mammals, J. Archaeol. Sci., 32, 1459–1470, https://doi.org/10.1016/j.jas.2005.03.015, 2005.

Zazzo, A., Bendrey, R., Vella, D., Moloney, A. P., Monahan, F. J., and Schmidt, O.: A refined sampling strategy for intra-tooth stable isotope analysis of mammalian enamel, Geochim. Cosmochim. Acta, 84, 1–13, https://doi.org/10.1016/j.gca.2012.01.012, 2012.